Department of Forest Products Technology

Studies on the ultrastructure of natural fibres and its effects on the fibre utilization

Tuomas Hänninen

Aalto University

DOCTORAL DISSERTATIONS

Aalto University publication series
DOCTORAL DISSERTATIONS 116/2011

Studies on the ultrastructure of natural fibres and its effects on the fibre utilization

Tuomas Hänninen

Doctoral dissertation for the degree of Doctor of Science in Technology to be presented with due permission of the School of Chemical Technology for public examination and debate in Auditorium Puu2 at the Aalto University School of Chemical Technology (Espoo, Finland) on the 11th of November 2011 at 12 o'clock.

Aalto University
School of Chemical Technology
Department of Forest Products Technology
Wood Chemistry

Supervisor
Professor Tapani Vuorinen

Instructor
Dr. Eero Kontturi

Preliminary examiners
Dr. Umesh Agarwal, USDA Forest Service, USA
Prof. Ingo Burgert, Swiss Federal Institute of Technology Zürich, Switzerland

Opponent
Professor Callum Hill, Edinburgh Napier University, UK

Aalto University publication series
DOCTORAL DISSERTATIONS 116/2011

ISBN 978-952-60-4359-3 (pdf)
ISBN 978-952-60-4358-6 (printed)
ISSN-L 1799-4934
ISSN 1799-4942 (pdf)
ISSN 1799-4934 (printed)

Unigrafia Oy
Helsinki 2011

Finland

The dissertation can be read at http://lib.tkk.fi/Diss/

Author
Tuomas Hänninen

Name of the doctoral dissertation
Studies on the ultrastructure of natural fibres and its effects on the fibre utilization

Publisher School of Chemical Technology

Unit Department of Forest Products Technology

Series Aalto University publication series DOCTORAL DISSERTATIONS 116/2011

Field of research Wood Chemistry

Manuscript submitted 24 October 2011 **Manuscript revised** 24 October 2011

Date of the defence 11 November 2011 **Language** English

☐ **Monograph** ☒ **Article dissertation (summary + original articles)**

Abstract

The ultrastructure of plant fibers has a significant effect on the properties of plants as well as on the behavior of the plant material undergoing various processing conditions, which logically affects the the final applications of plant-based materials. In this thesis, the ultrastructure of natural fibres was analysed using several complementary techniques to gain new insights into the ultrastructure of both wood and non-wood fibres.

The hierarchical structure of the natural fibre cell wall was found to play a vital role in cell wall reactivity and the material properties of fibres. Fibre defects, disruptions in the cell wall hierarchy, were found to have significantly increased susceptibility to chemical reactions when compared to intact fibre sections. An increase in the amount of defects was also found to slightly decrease the fibre strength properties. Another hierarchical feature, the microfibril angle was found to govern several properties of fibres and wood material. High strain to failure could be seen in both paper handsheets and samples of juniper wood, a species with a high microfibril angle. The effect of microfibril angle overrides the effects of chemistry and fibre dimensions when explaining the fibre properties.

The distribution of the cell wall components were, in fact, found to be similar in all of the wood species analysed. However, differences could be found in the distribution of lignin functional groups between spruce and pine. Differences in coniferyl aldehyde group distributions were seen also in size exclusion chromatography measurements of isolated lignin samples. Such deviation between pine and spruce was used to explain the differences in their behaviour during thermomechanical pulping.

Size exclusion chromatography also revealed differences in the ultrastructures of similarly processed eucalyptus and birch pulps. Eucalyptus pulp was found to have considerable amounts of lignin associated with the cellulose fraction of the pulp, whilst in birch most of the lignin was associated with hemicelluloses. Such differences can be of use when optimizing bleaching processes to decrease the consumption of chemicals.

Keywords Ultrastructure, natural fibres, wood, bast fibres, defects, Raman imaging

ISBN (printed) 978-952-60-4358-6 **ISBN (pdf)** 978-952-60-4359-3

ISSN-L 1799-4934 **ISSN (printed)** 1799-4934 **ISSN (pdf)** 1799-4942

Location of publisher Espoo **Location of printing** Helsinki **Year** 2011

Pages 164 **The dissertation can be read at** http://lib.tkk.fi/Diss/

Aalto-yliopisto

Tiivistelmä

Aalto-yliopisto, PL 11000, 00076 Aalto www.aalto.fi

Tekijä
Tuomas Hänninen

Väitöskirjan nimi
Luonnonkuitujen hienorakenteet ja niiden vaikutus kuitujen käyttömahdollisuuksiin

Julkaisija Kemian tekniikan korkeakoulu

Yksikkö Puunjalostustekniikan laitos

Sarja Aalto University publication series DOCTORAL DISSERTATIONS 116/2011

Tutkimusala Puukemia

Käsikirjoituksen pvm 24.10.2011 **Korjatun käsikirjoituksen pvm** 24.10.2011

Väitöspäivä 11.11.2011 **Kieli** Englanti

☐ **Monografia** ☒ **Yhdistelmäväitöskirja (yhteenveto-osa + erillisartikkelit)**

Tiivistelmä

Luonnonkuitujen hienorakenteella on vaikutusta niin kasvien ominaisuuksiin kuin niiden käyttömahdollisuuksiin teollisissa prosesseissa. Kuitujen hienorakenne voi vaihdella eri lajien välillä, ulkoisten ärsykkeiden seurauksena tai erilaisten käsittelyjen seurauksena.

Luonnonkuitujen rakenteellinen hierarkia vaikuttaa merkittävästi niin kuitujen kemialliseen reaktiivisuuteen kuin niiden materiaaliominaisuuksiin. Kuidun seinämien vaurioituneiden osien havaittiin olevan ehjiä osia huomattavasti alttiimpia kemiallisille reaktioille. Vaurioiden määrän havaittiin myös heikentävän kuitujen lujuusominaisuuksia. Myös mikrofibrillikulman voitiin todeta vaikuttavan merkittävästi kuitujen ja puun ominaisuuksiin. Katajasta valmistetut puu- ja paperinäytteet olivat hyvin elastisia, minkä katsottiin johtuvan katajan hyvin suuresta mikrofibrillikulmasta. Mikrofibrillikulman vaikutuksen kuitujen ja puun ominaisuuksiin havaittiin olevan huomattavasti kemiallisia eroja suurempi.

Eri puulajien välillä ei voitu havaita eroja niiden rakenteellisten komponenttien jakaumissa. Kuusessa ja männyssä voitiin kuitenkin havaita eroja eri soluseinien ligniinien koniferyylialdehydi-jakaumissa, mikä voitiin vahvistaa kokoekskluusiokromatografian avulla. Eroavaisuuksilla voidaan mahdollisesti selittää kuusen ja männyn eroavaisuuksia niiden kuituuntumisessa kuumahierreprosessissa.

Kokoekskluusiokromatografia myös paljasti eroja happivalkaistujen koivu ja eukalyptus massojen hienorakenteissa. Koivussa suurin osa ligniinistä oli sitoutunut massan hemiselluloosafraktioon kun taas eukalyptuksessa ligniiniä löytyi eniten selluloosafraktiosta. Ligniinin sitoutumisella eri hiilihydraattifraktioihin saattaa olla suuri merkitys eri puulajeista valmistettujen massojen valkaisussa.

Avainsanat Hienorakenteet, luonnonkuidut, puu, niinikuidut, kuituvauriot, Ramankuvantaminen

ISBN (painettu) 978-952-60-4358-6 **ISBN (pdf)** 978-952-60-4359-3

ISSN-L 1799-4934 **ISSN (painettu)** 1799-4934 **ISSN (pdf)** 1799-4942

Julkaisupaikka Espoo **Painopaikka** Helsinki **Vuosi** 2011

Sivumäärä 164 **Luettavissa verkossa osoitteessa** http://lib.tkk.fi/Diss/

Preface

This study was carried out at the Department of Forest Products Technology at Helsinki University of Technology, now known as Aalto University during 2007-2011. Work was done as part of the projects supported by Nordic Energy research (NER), Multidisciplinary Institute of Digitalisation and Energy (MIDE) and European Community's Seveth Framework Programme (FP7/2007-2013).

I am grateful to Professor Tapani Vuorinen for giving me the opportunity to work under his supervision. I am thankful for his guidance and for the freedom he gave me during my studies. My instructor, Eero Kontturi is acknowledged for his support since 2005. It has been a great pleasure to work with such an ingenious and hardworking scientist.

Professor Mark Hughes I thank for welcoming a chemist into wood technology research group, giving me responsibilities in the projects and showing me also their bureaucratic side. I am grateful for having an opportunity to work with all of my co-authors from Tokyo University, Technical University of Denmark, Metsäntutkimuslaitos METLA and Helsinki University. I want to especially thank Professor Akira Isogai and Assistant Professor Tsuguyuki Saito for giving me the spark to start my doctoral studies.

Many thanks for all of my friends and colleagues in the Department of Forest Products Technology for creating a pleasant environment to work in. Without colleagues like Tiina, Elli, Laura, Hannes, Niko, Mikhail, Miro, Katri, Karoliina, Delphine, Pekka and Lauri, life in the lab would have been much duller. I thank the technical staff, Risu, Aila, Anu, Rita and Marja for assistance in laboratory. Timbe deserves special thanks for help in the laboratory and for intriguing discussions at work and elsewhere. Department's former librarian Kati Mäenpää I thank for the assistance in acquisition of numerous scientific publications and for the help keeping the coffee break tradition alive even when the others were far away. Tekla and Jaakko from VTT are thanked for encouraging me to do something completely different during my studies.

I thank all the members of “Teh Band”, former and current, for having a chance to produce noise we called music with you and for providing me an escape from the dull everyday routines. Big thanks also belong to “Latter Hour Saints” and all the participants of the shadow banquets for providing invigorating company and lively discussions during the conferences.

I thank my friends outside the work community, especially my “honorary brothers” who have indeed been like brothers to me, for keeping me in touch with the nonscientific side of life. Markku Jouppila is thanked for all the refreshing lunch breaks. My whole family is acknowledged for supporting me during my doctoral studies. Without your love and encouraging I never would have made it so far. I also thank Tanja for her support and for waiting patiently until the thesis was finished.

Last, but not least, I thank Nalle for all the unconditional love and for forcing me to take a refreshing walk outside every once in a while.

Espoo, 24th October 2011

Tuomas Hänninen

Table of Contents

List of publications

This thesis is mainly based on the results presented in six publications, which are referred to as Roman numerals in text. Thesis contains also additional unpublished data related to the work.

Paper I Hänninen, T., Michud, A., Hughes, M. (2011) Kink bands in bast fibres and their effects on mechanical properties. Plastics, Rubber and Composites, 40(6-7):307-310.

Paper II Hänninen, T., Thygesen, A., Mehmood, S., Madsen, B., Hughes, M. (2011) Mechanical processing of bast fibres: the occurrence of damage and implication for fibre structure. (Submitted)

Paper III Hänninen, T., Tukiainen, P., Svedström, K., Serimaa, R., Saranpää, P., Kontturi, E., Hughes, M., Vuorinen, T. (2011) Ultrastructural evaluation of compression wood-like properties of *Juniperus communis*. Holzforschung (Accepted)

Paper IV Hänninen, T., Kontturi, E., Leppänen, K., Serimaa, R., Vuorinen, T. (2011) Kraft Pulping of *Juniperus communis* Results in Paper with Unusually High Elasticity. Bioresources 6(4), 3824-3835.

Paper V Hänninen, T., Kontturi, E., Vuorinen, T. (2011) Distribution of lignin and its coniferyl alcohol and coniferyl aldehyde groups in *Picea abies* and *Pinus sylvestris* as observed by Raman imaging. Phytochemistry, 72:1889-1895.

Paper VI Hänninen, T., Kontturi, E., Isogai, A., Vuorinen, T. (2008) Differences in residual lignin properties between *Betula verrucosa* and *Eucalyptus urograndis* kraft pulps. Biopolymers 89(10):889-893

Author's contributions:

I-II Tuomas Hänninen was responsible for the research plan, experimental design, performing some of the analyses and preparation of the manuscripts.

III Tuomas Hänninen was responsible for the research plan, experimental design, acquisition of the samples, chemical analyses, Raman imaging and preparation of the manuscript.

IV Tuomas Hänninen was responsible for acquisition of the samples, experimental design, sample preparation, chemical analysis, handsheet testing and preparation of the manuscript.

V Tuomas Hänninen was responsible for experimental design, Raman imaging and preparation of the manuscript.

VI Tuomas Hänninen was responsible for experimental design, sample preparation, SEC analysis and preparation of the manuscript.

List of Abbreviations:

CAA	Coniferyl alcohol and aldehyde
CAld	Coniferyl aldehyde
CAlc	Coniferyl alcohol
DP	Degree of polymerization
ESCA	Electron spectroscopy for chemical analysis
HMW	High molecular weight
LMW	Low molecular weight
LCC	Lignin-carbohydrate complex
LODP	Level-off degree of polymerization
MALS	Multi-angle laser light scattering
MFA	Microfibril angle
RI	Refractive index
SEM	Scanning electron microscopy
TMP	Thermomechanical pulping
XRD	X-ray diffraction

1. Introduction and outline of the work

Studies on the chemistry and ultrastructure of natural fibres are presented in this thesis. The aim of the thesis is to increase knowledge about several ultrastructural features which are generally considered to hinder the industrial application of natural fibres and to obtain more knowledge on the natural fibre composite structure. It focuses on the heterogeneity of the natural fibres and the requirements it sets to the processes using them as raw material. The heterogeneity can be the result of fibre processing (papers I, II and VI) or it is present as natural differences between species (papers III-VI). Understanding the diversity of natural fibres as a material not only enables us to improve existing processes but to also help us design better man-made materials by mimicking nature.

This work has involved several projects whose topics ranged from the modelling of wood to enhancing the properties of bast fibres for textile production and for natural fibre composites.

Defects caused by the processing of bast fibres were investigated and reported in papers I and II. Defects were shown to be more susceptible to the chemical reactions, which in turn might cause problems in the utilization of the fibres in composite applications due to heterogeneity in the fibre chemistry and structure. Defects were also observed to weaken the mechanical properties of the fibres.

Papers III and IV focus more on the elastic properties of fibres and how these are manifested at the wood material level. Pulping experiments of juniper revealed its highly elastic fibre properties, which also could be seen in 4-point bending tests on juniper wood. The chemical composition, chemical distribution and fibre analyses revealed that the high microfibril angle of juniper fibres was the determining factor for its material properties.

No differences in the lignin/cellulose distributions of any of the species analysed could be observed, however, paper V shows that small differences in the distribution of lignin functional groups could play an important role in industrial processes. Clear differences could be seen in the distributions of coniferyl alcohol and coniferyl aldehyde groups of the lignin in different wood species. Additional size exclusion chromatography measurements also backed-up these findings. Such differences were used to explain the dissimilar behaviour of pine and spruce in thermomechanical pulping.

Size exclusion chromatography was also used in paper VI, which demonstrates differences in the lignin distribution with respect to the carbohydrates in birch and eucalyptus kraft pulps. Lignin in birch pulp was mainly associated with hemicelluloses because a significant fraction of lignin in eucalyptus was observed in the cellulose fraction. Such differences can be closely associated with chemical consumption in the removal of residual lignin by bleaching.

2. History of natural fibre products

In one form, a composite is a solid material composed of plastic matrix with an embedded fibrous material. Wood could be considered to be a natural fibre composite or even a nanocomposite, which has been in use ever since man learned how to use tools. The composite analogy works for natural fibres at two scales. A single fibre can be considered a nanocomposite where nano-sized cellulose microfibrils are embedded in a matrix of lignin and hemicelluloses, while the whole plant can be considered a natural fibre composite where micron-sized fibres are embedded in a continuous lignin matrix, i.e., middle lamella.

Natural fibres have been used by men in composites since the dawn of civilization. The earliest known man-made natural fibre composites date back to 10 000 B.C. in China, where shards of pottery containing hemp fibres have been found (Rowell, 2008). There are also Biblical references that show ancient Egyptians using straw to reduce the cracking of clay bricks (Exodus, Chapter 5).

World's most widely used and widespread natural fibre composite, paper, was invented in China around 105 A.D. Old rags and plant tissue were used as the material for paper sheets. Papermaking spread slowly westwards and reached Europe in the 11th century. By the 14th century, several paper mills existed in Europe and they were using linen, hemp and cotton rags as the raw material. In the 1850s the first commercial mechanical pulping machine using wood as the raw material was developed. However, it took until the 1870s for the method to be used extensively when a steam pretreatment to soften the fibre binding matrix was introduced to the process. The first chemical pulping process, an acidic soda process, was introduced in 1851 and the most common process used today, kraft pulping, was developed in 1884 (Sixta, 2008). Research in the pulp and papermaking field has been very active ever since and new processes are still being designed to improve the quality of products produced from different wood species.

In the field of composites, the first applications arose in the 1850s, before the first modern resins and plastics were invented. In America, shellac mixed with wood flour was used to produce union cases used for displaying early photographs. At around the same time in France, a composite prepared from albumen and wood flour, called “Bois durci”, i.e., hardened wood, was patented (Hänninen and Hughes, 2010).

The age of modern composites began with the invention of Bakelite, the first fully synthetic thermosetting resin, in 1907. Since Bakelite is brittle, it was reinforced with fillers, such as wood flour to improve its properties. In the 1930s in particular, pioneering work was carried out in the field on natural fibre composites to produce composite materials for aeronautics (Hänninen and Hughes, 2010).

With the commercialization of glass fibre in the 1940s interest in natural fibre composites declined. More or less regularly efforts to produce natural fibre composites for decorative and structural applications occurred thereafter. However, until today there have been only a few structural applications that have been commercially successful (Hänninen and Hughes, 2010). One of the reasons for the poor performance of the natural fibres as a reinforcing fibre in composites could be the old defibration processes that date back hundreds of years.

Wood, however, has succeeded where man-made composites have failed. Wood is widely used in magnificent structures such as Sakyamuni Pagoda in China, the tallest wooden structure in the world. By understanding the ultrastructural features of natural fibres, we can get closer to producing equally good composites. Knowledge about ultrastructure of fibres will also aid us in the utilization of the natural fibre resources.

Comprehension of the ultrastructure of natural fibres not only aids us in optimizing existing processes, such as the pulping and bleaching of wood fibres, but it can also give us insight to develop totally new kinds of processes to replace old ones. New approaches are indeed needed, especially in the field of natural fibre reinforced composites, where the product properties are not able to compete with man-made fibre reinforced composites and their driving force, environmental friendliness, has been recently seriously questioned (Dissanayake et al., 2009a, Dissanayake et al., 2009b)

3. Structure of natural fibres

Although plants consist of many different kinds of cells, which serve their specific purpose in the plant, mainly the load bearing cells are used in industry. The wood fibres that are utilized in pulp and paper are so called xylem fibres or tracheids. A schematic image of pine xylem section is illustrated in Figure 1.

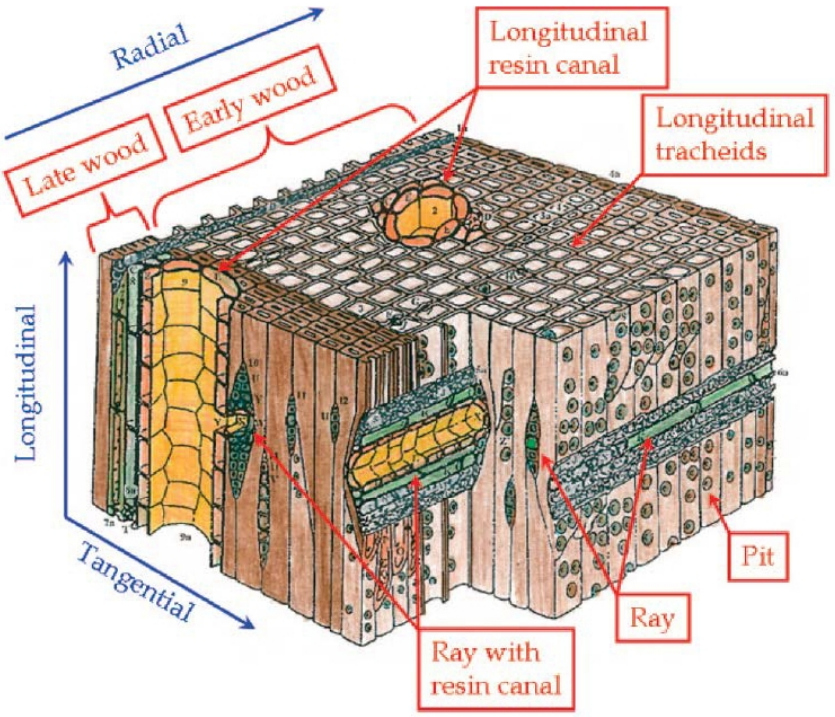

Figure 1. Structure of pine xylem (Kekkonen et al., 2009).

Other important fibre type that are utilized industrially are phloem, or bast fibres. Although trees also contain bast fibres, their utilization is minimal. The use of bast fibres from the stems of annual plants such as hemp and flax, is much more common. The bast

fibres are arranged in bundles several fibres thick (Eder and Burgert, 2010), which can be seen from the Figure 2 illustrating cross-section of flax stem.

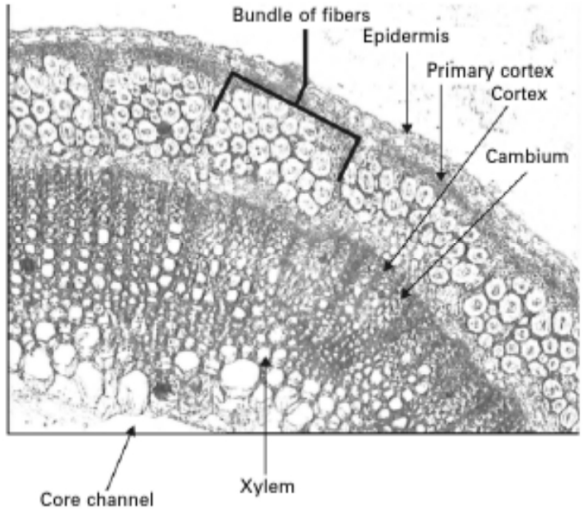

Figure 2. Cross-sections of a flax stem (Blackburn, 2005).

Natural fibres are a very challenging raw material to use due to their heterogeneous nature. Although natural fibres are in general composed of the same chemical compounds and their hierarchical cell wall structure is very similar, significant differences in fibres can be found within the same species, or even within the fibres growing in the same plant.

Natural fibres are analogous to a nanofibre composite composed of cellulose microfibrils functioning as the reinforcing fibres embedded in matrix of lignin and hemicelluloses. In addition other compounds, such as waxes, fats and extractives can be found in plants (Sjöström, 1993). However, they will not be discussed in this thesis due to their minor structural role within the cell wall.

3.1 Cellulose

Cellulose, which is possibly the most studied component of plants due its abundance in nature, is a linear polymer of variable length consisting of 1-4-linked β-D-anhydroglucopyranose units. Every second anhydroglucose unit is rotated through 180° with respect to the adjacent unit meaning that the actual repeating unit in the cellulose polymer is cellobiose, as illustrated in Figure 3.

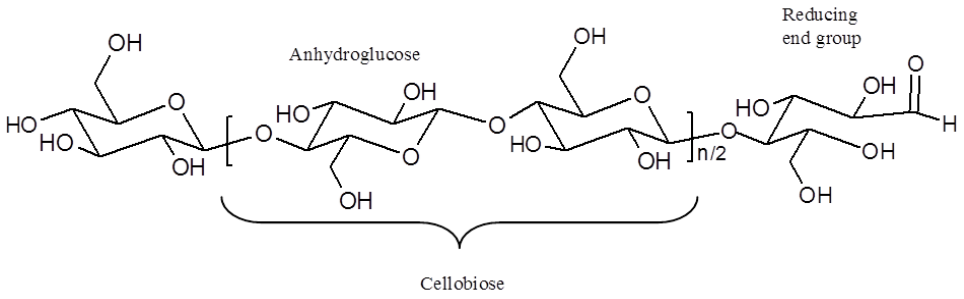

Figure 3. Structure of cellulose.

In nature, cellulose molecules can be found in microfibrils, agglomerates of several cellulose chains bound together by a tight intermolecular hydrogen bond network. The quantity as well as the length of the cellulose molecules in a single microfibril depends on the botanical source (Davidson et al., 2004).

Cellulose in its native state is organized in a crystalline form called cellulose I. In cellulose I the cellulose chains are packed in a parallel arrangement. The cellulose chains are bonded together with hydrogen bonds between the hydrogen of the OH-group in the sixth position and oxygen of the hydroxyl group in the third position of another chain, which is considered to be the most important one for cellulose I from the chemical point of view (Klemm et al., 2004).

In 1980s Atalla and VanderHart published studies (Atalla and VanderHart, 1984, VanderHart and Atalla, 1984) where crystalline allomorphs of cellulose I_α and I_β were

introduced. According to these authors cellulose I_α was the dominant form in cellulose obtained from bacterial sources while in ramie, cotton or wood cellulose I_β was dominant.

The structure of the cellulose microfibril is not considered to be uniform throughout the fibril. A two-phase model introduced by Mark (1940) assumed that microfibrils consist of highly ordered crystalline and disordered amorphous regions. This model is better known as the fringed fibrillar model according to Hearle (1958) and it is the established model today (Nishiyama et al., 2003).

The exact crystalline arrangement of cellulose is still under debate. In some studies a paracrystalline model has been proposed, where a large proportion of disordered cellulose is located on the surface of the crystals (Viëtor et al., 2002, Leppänen et al., 2009). In a model proposed by Salmén and Bergström (2009) disordered regions are found on the surface and inside the cellulose microfibrils. Recently, Atalla has proposed that the native state of cellulose is none of the proposed forms and crystalline and amorphous regions in microfibrils is only an artefact caused by the isolation technique of the microfibrils or the harsh measurement conditions (Atalla et al., 2009).

3.2 Hemicelluloses and pectins

In contrast to highly ordered cellulose, hemicelluloses are branched heteropolymers with a low degree of polymerization (DP) and no crystallinity. Hemicelluloses can be built up from various monomeric units, for example glucose, mannose, galactose, arabinose, xylose as well as from small amounts of uronic acids such as 4-O-methylglucuronic acid and D-galacturonic acid (Sjöström, 1993). The structure of xylan, the most abundant hemicellulose in hardwoods, is illustrated in Figure 4. In the cell wall hemicelluloses act as the binding material between microfibrils enabling the mobility of microfibrils in deformation (Keckes et al., 2003). It has also been proposed that hemicelluloses take part in orienting cellulose microfibrils during the biosynthesis of cellulose (Reis and Vian, 2004).

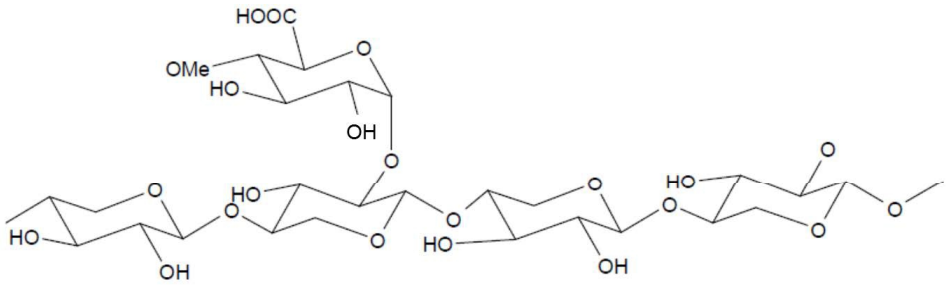

Figure 4. Structure of xylan with 4-O-methylglucuronic acid group.

Pectins are sometimes considered hemicelluloses due to their similar structure. Like hemicelluloses, pectins are amorphous and most of them are branched heteropolymers. Various pectic polysaccharides have been detected in the cell wall, including homogalacturonan, rhamnogalacturonan I, rhamnogalacturonan II, arabinan, arabinogalactan and galactan (Meshitsuka and Isogai, 1996).

3.3 Lignin

Lignins are complex heteropolymers derived mainly from three hydroxycinnamyl alcohol monomers with differing degrees of methoxylation; *p*-coumaryl, coniferyl and sinapyl alcohols which are illustrated in Figure 5. These monomers produce respectively *p*-hydroxyphenyl (H), guaiacyl (G) and syringyl (S) units when incorporated into the lignin polymer. The amount and composition of lignin varies greatly between species. Generally, it is thought that hardwood lignin consist of G and S units whilst softwood lignin is composed almost solely of G units. The H units have been considered to be found mainly in grasses (Sakakibara and Sano, 1996). Although lignin is conventionally considered to consist of these three main precursors, many plants contain significant levels of other precursors (Sederoff et al., 1999), for example coniferaldehyde structures.

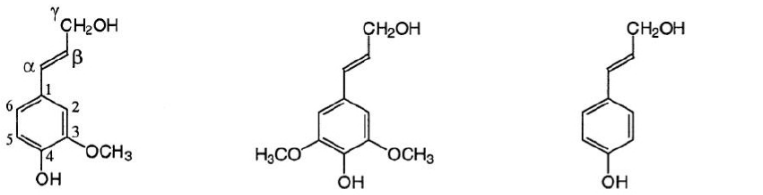

trans-Coniferyl alcohol *trans*-Sinapyl alcohol *trans-p*-Coumaryl alcohol

Figure 5. Structures of the main lignin precursors.

The function of lignin in the plant cell wall is to act as cementing material to other structural units as well binding cells together. Lignin also provides compression strength and stiffness to cells and due to its hydrophobic nature, it also controls the water content of the cell wall and enables cells to transport water. There have also been reports of lignin's role in protecting plants against pathogens (Boerjan et al., 2003).

Lignin is thought to form linkages with cell wall polysaccharides. The presence of lignin-carbohydrate complexes (LCCs) has been under debate after their proposed discovery by Björkman (1956). However, several studies are pointing towards their existence in pulp and in wood (Henriksson et al., 2007, Lawoko et al., 2005, Li et al., 2011). LCCs have been considered to be one of the reasons for the difficulties to encountered in removing the residual lignin from pulp during bleaching (Henriksson et al., 2007). Lignin has been considered to form linkages mainly with hemicelluloses, but there has also been speculation about lignin-cellulose linkages (Jin et al., 2006, Tenkanen et al., 1999).

3.4 Structure of plant cell wall

Although the functions of plant cells may vary, their structure is very much alike. Natural fibres are constructed so that the innermost and load bearing secondary cell wall surrounds the hollow center of the fibre, the lumen. The outermost cell wall is called the primary cell wall and between the cells resides the fibre binding middle lamella. The secondary cell wall can be further divided into smaller layers according to the

arrangement of microfibrils, for example, into layers S3, S2 and S1 in the case of wood cells (Figure 6). Some studies have proposed that in flax and hemp the S2 layer could be divided to even smaller layers (Blake et al., 2008, Romhány et al., 2003, Charlet et al., 2010).

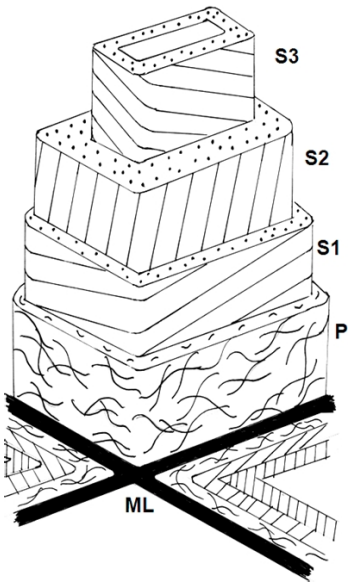

Figure 6. Schematic representation of the structure of wood cells. Individual cells are separated by middle lamella. The cell wall is divided into two layers, primary wall (P) next to middle lamella (ML) and secondary wall which is further divided in S1, S2 and S3 layers. A hollow lumen is surrounded by the cell wall layers.

The S2 is the dominant cell wall layer when it comes to the physical properties of processed fibre or unprocessed plants like wood. In general, the S2 is the thickest cell wall layer and therefore the orientation of the microfibrils and the chemical structure in this layer affects the material properties most. the S1 and S3 cell walls have been proposed to strengthen the cell against deformation by swelling with water, as well as contributing to the lateral hardness and crushing strength of timber (Donaldson, 2007, Bergander and Salmén, 2002).

Although there are some distinctions in the chemical compositions of different plants, the different cell wall layers resemble each other. The secondary cell wall has a very high cellulose content, although in wood also significant amounts of lignin and hemicelluloses are present. Salmén and Olsson (1998) have shown that in the cell wall of spruce fibres, different hemicelluloses were associated with different cell wall components. Galactoglucomannan was found to be attached to the surface of cellulose fibrils while xylan was more associated with lignin. Terashima et al. (2009) have proposed a model for the assembly of the cell wall components in the secondary cell wall of ginkgo (Figure 7a) where cellulose microfibrils are aggregated in bundles of different sizes which are encrusted with hemicelluloses and subsequently bound together by lignin-hemicellulose complexes. A similar model has also been proposed by Fahlén and Salmén (2004), which is illustrated in Figure 7b. It has been shown that the lignin content affects the size of these cellulose microfibril bundles (Donaldson, 2007). In hemp and flax fibres, only small amounts of lignin have been detected in the secondary cell wall. In flax and hemp, the microfibril bundles are surrounded by pectins and small amounts of proteins in addition to lignin and hemicellulose (Blake et al., 2008, Gorshkova et al., 2000, Day et al., 2005).

The chemical composition of the cell wall changes greatly during the development of the cell. For example, in a wood cell, carbohydrates are initially present in the cell wall and lignin starts to form later (Sjöström, 1993). The primary cell wall and the middle lamella of a cell contain the highest concentrations of lignin when the cell has reached its fully grown state in both wood and bast fibres. In wood the main component of the primary cell wall and the middle lamella is lignin while in bast fibres, pectic compounds also play a major role. A thorough understanding of the composition of the middle lamella is essential when considering the isolation of the fibres. Considerable efforts have been expanded in the characterization of the middle lamella in wood, while only recently studies on the chemical distributions in hemp and flax have started to emerge.

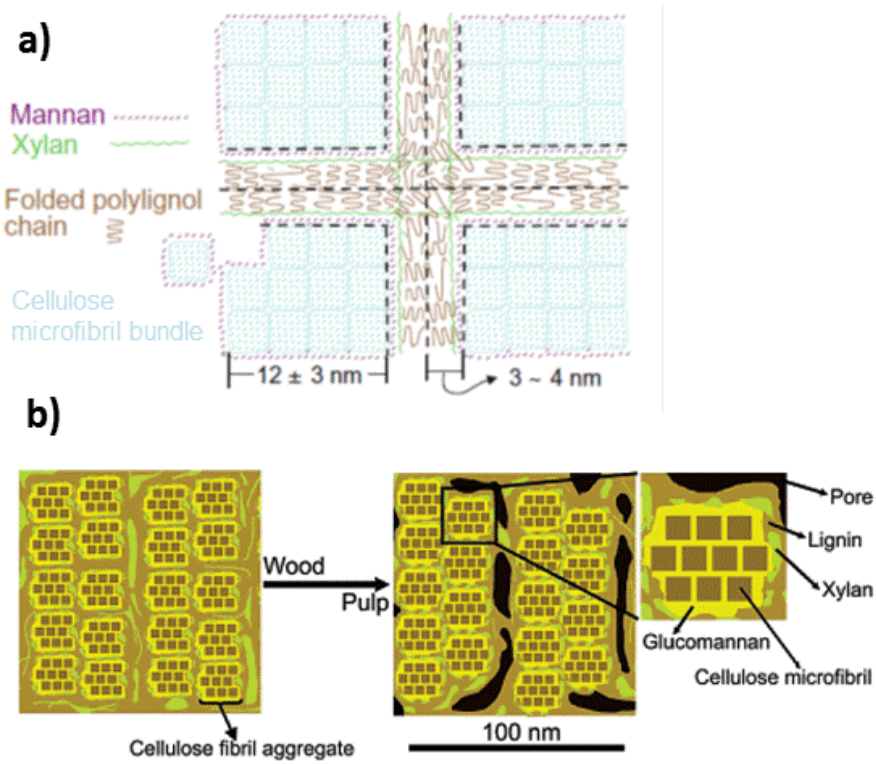

Figure 7. Schematic illustrations of S2 cell wall layer structure by (a) Terashima (2009) and (b) Fahlén and Salmén (2004).

4. Role of artificially induced defects in natural fibres

The structural integrity of the plant cell wall plays a very important role in applications of natural fibres, especially when compared to man-made fibres which can be considered to be practically free of defects. Fibres obtained from plants always contain defects. The defects can occur due to the functions of the fibre, for example pits that enables water conduction between adjacent cells.

Fibres also contain defects caused by mechanical action. These kinds of defects are also known as kinks, kink bands, microcompressions or nodes, among others. Micrographs of such defects in processed and unprocessed flax fibres are illustrated in Figure 8.

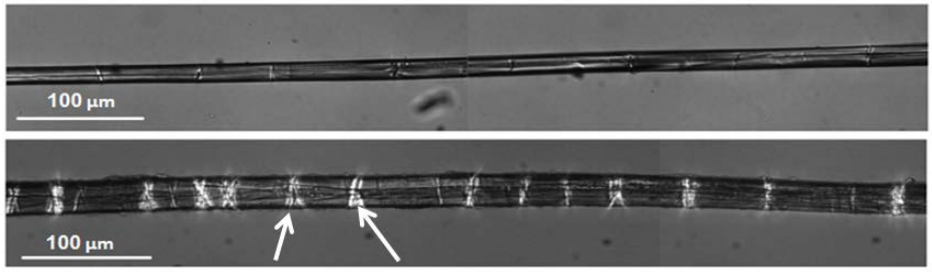

Figure 8. Micrographs by polarized light microscope of unprocessed (upper) and processed hemp fibres. Some of the defects are pointed out by arrows. (Paper II)

4.1 Effect on mechanical properties

The effect of defects on the mechanical properties of fibres has long been under debate. Although the results are contradictory, it can be concluded with a fair degree of certainty that defects do affect tensile properties (Page et al., 1972, Davies and Bruce, 1998, Thygesen et al., 2007, Baley, 2004). This can also be seen from the fibre strength data in Table 1. Although there is a decrease in tensile strength values when comparing

processed fibres with unprocessed ones, the values are within standard deviation, and thus the significance of the difference can be questioned.

Table 1. Flax fibre properties from single fibre tensile tests. (Paper I)

	Diameter (μm)	Tensile strength (MPa)	Elastic modulus (GPa)	Max load (N)
Fresh Flax	35.2 ±7.3	322 ±93	15.9 ±6.9	0.29 ±0.009
Retted Flax	17.3 ±3.6	486 ±168	24.1 ±7.6	0.12 ±0.06
Flax Noils	26.6 ±5.4	344 ±114	17.6 ±7.5	0.20 ±0.09
Cottonized Flax	28.2 ±4.4	306 ±85	17.7 ±5.6	0.20 ±0.07

The tensile strength of fibres extracted from fresh stems is lower than that of fibres extracted from retted stems. As retting most probably does not increase the fibre strength, the cross-sectional area of the fibres, which is used in calculations on the tensile strength values must be taken into account. The huge variations in fibre diameter, especially between fibres extracted from fresh and retted stems, is the most likely cause of artefacts in strength property measurements. Fresh fibers might corporate the remainder of middle lamella, which may lead to measurement errors using optical microscopy. Using a standard transmitted light microscope will lead to error in the in the determination of the actual cross-sectional area of the fibres, since it measures the fibre for only one side. To enable the acquisition of the true cross-sectional area of the fibre, confocal microscopy should to be used.

Table 2. Hemp and flax fibre properties (Müssig et al., 2010)

	Tensile strength (MPa)	Young's modulus (GPa)	Elongation at break (%)	Diameter of single fibre (μm)
Flax	343-1500	8-100	1.2-4	1.7-76
Hemp	310-1110	3-90	1.3-6	3-51

The diameter of the fibres is not the only variable that causes error in single fibre tensile property measurements. To mention a few other examples, clamping length, testing speed, and the relative humidity affect the results. As seen from Table 2, the variations

between the single fibre test values differ greatly in the literature (Müssig et al., 2010). To compare natural fibre strength data, one would need better standardized equipment and methods. Paper handsheet tests are good examples of well standardized methods.

4.2 Effect of defects on the susceptibility of fibres to acid hydrolysis

The defects do not only decrease the strength properties of the fibres, but they are also more susceptible to chemical reactions (Rauvanto et al., 2006, MacLeod, 1990). Inhomogeneous reactivity along the fibre may cause problems, for example, during fibre modifications, when intact parts of the fibres may remain unmodified while the defects are weakened.

In this work (Paper II), the susceptibility of the defects to hydrolytic degradation was used to aid determination of the defects. The quantification of defects using polarized light microscopy is very tedious work and the bast fibres are unsuitable for most of the automatic fibre analysers, such as FiberLab, because of their long fibre length. A method, where the defects are weakened by acid hydrolysis with subsequent mechanical breaking of the fibres has been used to render bast fibres suitable for analysis by automatic instruments. Mechanical breakage, however, tends to cleave the fibres in the undefected parts of the fibre as well.

Mild acid hydrolysis in combination with viscosity measurements was used to analyse the susceptibility of defects in bast fibres to acid hydrolysis. Viscosity measurement is a used routinely in analytical technique employed pulp testing to evaluate the chemical damage to fibres. The theory of the viscosity measurements is discussed in Experimental sections of this thesis.

Table 3. Chemical composition and intrinsic viscosity before and after acid hydrolysis of industrial flax and laboratory damaged hemp fibres. The defected area determined by polarized light microscopy is reported for flax only. The extent of damage is reported as the function of number of passes through cog wheels for hemp. (Paper II)

Untreated fibres								
Flax		Cellulose (%)	Hemicellulose (%)	Lignin (%)	Pectin (%)	Other (%)	Intrinsic Viscosity (ml/g)	Defected area (%)
	Green stem	59	9	3	8	7	1554	24.4±6.8
	Retted stem	70	12	2	5	3	1874	19.6±12.1
	Noils	79	8	2	2	3	2027	37.4±7.0
	Kotonina	79	7	4	5	2	2039	36.2±4.7
Hemp								
	0 passes	74	11	6	4	7	1600	
	5 passes	74	11	6	5	6	1617	
	12 passes	77	11	3	3	5	1702	
	22 passes	76	11	5	3	7	1767	
Acid hydrolyzed fibres								
Flax								
	Green stem	82	8	6	2	2	974	
	Retted Flax	82	7	4	5	3	1058	
	Flax Noils	84	7	3	4	2	399	
	Kotonina	84	8	4	2	1	487	
Hemp								
	0 passes	83	10	2	3	4	634	
	5 passes	83	10	2	3	2	626	
	12 passes	82	10	3	3	5	556	
	22 passes	82	9	5	3	2	548	

As cellulose is the main component of the fibres and its DP is significantly higher than the DP of the other cell wall polymers, cellulose is the dominant contributor in the viscosity measurements. This can be seen from the correlation between cellulose content and viscosity, which is illustrated in Figure 9. Viscosity data has also been used to determine the DP of cellulose and hemicelluloses in pulp samples when their concentrations are known (da Silva Perez and van Heiningen, 2002). The method however cannot be directly applied to bast fibres due to their high lignin and pectin contents.

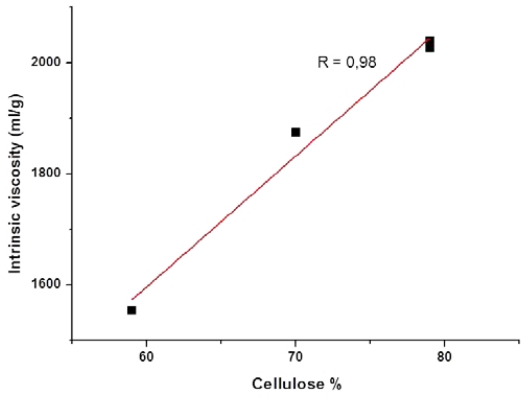

Figure 9. Relationship between the intrinsic viscosity and the cellulose content of untreated flax fibres. Standard deviation in the viscosity measurements was < 20. (Paper II)

When the viscosities after acid hydrolysis are plotted against the defected area of the fibres, a clear correlation can be seen (Figure 10). The decrease in viscosity after acid hydrolysis, when the defected area increases, clearly indicates that the susceptibility of the cell wall polymers to acid hydrolysis is increased in the defected areas. The defects in the structure enable acidic solutions to penetrate the cell wall where cellulose can be hydrolysed throughout the whole cell wall. The drastic drop in viscosity is caused by random cleavage of cellulose due to the acid hydrolysis.

Acid hydrolysis has also been used to determine the level-off DP (LODP) of cellulose (Battista, 1950), which has been shown to correlate with the average length of the crystalline region in cellulose microfibrils (Nishiyama et al., 2003). The determination of LODP is performed in very high acid concentrations and the decrease in viscosity is much greater than in method used in this work. For example, in the case of birch kraft pulp with 1000 ml/g viscosity reaches a LODP value at 200 ml/g (Håkanson et al., 2005).

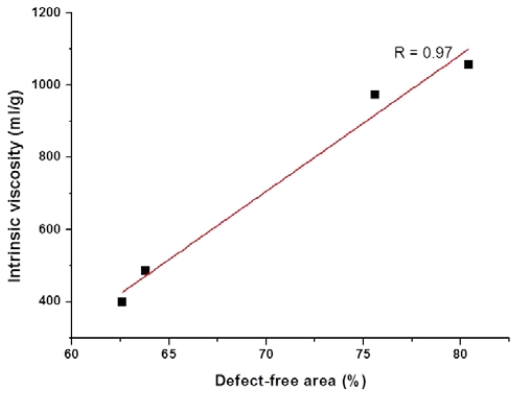

Figure 10. Relationship between the intrinsic viscosity and defect-free area of the acid hydrolysed flax fibres. Standard deviation in the viscosity measurements was < 20. (Paper II)

Interestingly, the decrease of viscosity after acid hydrolysis levels off after a certain amount of damage (Table 3). This leveling-off suggests that in a certain process, after a threshold degree of damage, the extent of damage introduced to the fibres is decreased significantly. A similar trend has also been reported by Rauvanto et al. (2006) for unbleached softwood pulp during PFI beating.

5. Assembly of the cell wall and its effects on the mechanical properties of fibres and wood

The same principles can be considered to apply to the properties of natural fibres as in any man-made composite. The outstanding properties of natural fibers lie in millions of years of product development, better known as evolution.

The alignment of the reinforcing fibre relation to the applied stress is one of the most important characteristics considering composite properties (Hull and Clyne, 1996). In the case of natural fibres, the microfibril angle (MFA) of the secondary cell wall can be considered to be the dominant factor when it comes to strength properties of the fibres (Donaldson, 2008).

The compression wood is known to differ from the normal wood by its chemistry and cell wall structure. Compression wood is formed as response to external stimuli to correct the growth direction of the tree and bring it back to the vertical. Uneven soil, heavy snow or strong winds are known to cause the formation of compression wood. Juniper (*Juniperus communis*), a small shrub-like conifer, is known for its exceptionally high strain to failure and it is commonly used by children as material for bows. Juniper, even with a straight trunk, is known to have several compression wood-like features, which makes it an interesting subject for ultrastructural research with respect to its material and fibre properties. In previous studies of high MFA wood species, usually only a few chemical analyses have been performed and the chemical distributions have not been determined from the samples. This leaves open the question; what role does the chemical distribution of cell wall components play in the mechanical properties of wood.

5.1 Analysis of juniper wood

Values from 4-point bending tests of spruce normal wood, spruce compression wood and juniper are presented in Table 4. The elastic modulus of juniper is indeed much lower than that of spruce normal wood. Juniper in fact resembles the compression wood of spruce in its mechanical properties. Another property of juniper that is reminiscent of compression wood is the high MFA, as seen in Table 5 and in the literature (Burgert et al., 2004, Kantola and Kähkönen, 1963, Kantola and Seitsonen, 1961).

Besides the MFA, density is one of the determining properties for the elasticity of wood. The increase in MFA decreases the elastic modulus while the increase in density increases it (Evans and Ilic, 2001, Yang and Evans, 2003, McLean et al, 2010). The densities of the spruce normal wood samples were 50 % lower than those of compression wood and juniper. Still the elastic modulus of juniper and compression wood was notably lower than that of the normal wood of spruce. Similar results have also been obtained for yew which also has a high MFA and high density (Keunecke et al., 2008).

Table 4. 4-point bending test data for spruce normal wood, spruce compression wood and juniper. (Paper III)

Sample name	Density (kg/m^3)	Modulus of elasticity (MPa)	Bending Strength (MPa)
Spruce normal wood	454 ±45	8605 ±915	74 ±5
Spruce compression wood	575 ±15	4962 ±439	93 ±3
Juniper	647± 118	4796 ±572	92 ±15

From the 4-point bending test data we can see that there is no correlation between the elastic moduli and densities of the samples. This indicates that in the case of these samples the MFA is the most dominant feature concerning the elasticity of these materials. Similar results as ours have been reported by Keunecke (2008) for yew. Denser samples could be observed to withstand higher stresses before breaking.

Crystal lengths were also similar in compression wood and juniper while spruce normal wood had clearly longer crystals (Table 5). Crystal length could also be one of the minor reasons for elasticity of juniper and compression wood. The shorter crystal length also implies an increase in the frequency of flexible amorphous regions in fibrils. As the fibril bundles in cell wall have then more flexibility (Page, 1983), this possibly reflects itself also to the fibre properties and further on to wood material properties, although the effect is likely to be so small that it is overplayed by more prominent features like MFA.

Although the crystal width in juniper was slightly smaller than in spruce normal wood and spruce compression wood (Table 5), values corresponded with the ones in literature which have rather large variation (Tanaka et al., 1981, Andersson et al., 2003, Davidson et al., 2003, Leppänen et al., 2009) and the difference was not considered to be significant relative to the mechanical properties of wood.

Juniper fibre morphology resembles more closely to compression wood fibres of spruce than normal wood fibres. Helical grooves in the S2 layer of cell wall, which are characteristic to compression wood, can be seen in the polarized light micrograph taken from juniper and compression wood samples (Figure 11).

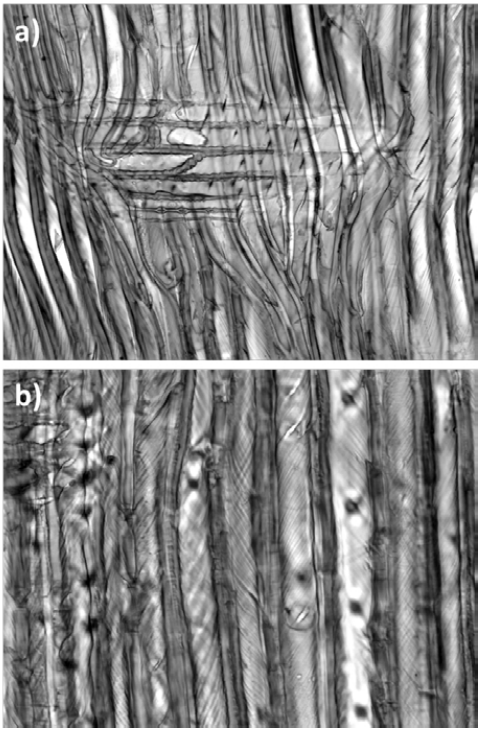

Figure 11. Radial sections of (a) common juniper and (b) compression wood of spruce. Helical grooves or cavities indicating the MFA of the cell wall are clearly visible. (Paper III)

Table 5. Microfibril angle in S2 cell wall layer, crystal length and width determined by using XRD. The standard deviation of the MFA values is presented within the brackets. The error margins for the dimensions of the crystallites are based on the accuracy of the measurement and analysis. (Paper III)

	MFA of S2 cell wall (degree)	Crystal length (nm)	Crystal width (nm)
Spruce normal wood	0.2 (7)	40±5	3.08±0.05
Spruce compression wood	35 (8)	20±2	3.06±0.05
Juniper	35 (9)	21±2	2.92±0.05
Juniper kraft pulp		16±2	4.0±1.0

In some respects the composition of juniper resembles that of spruce compression wood. The lignin and hemicellulose contents are higher in juniper (Table 6 and Table 7) than in the normal wood of spruce, but is lower than that of spruce compression wood. However, the carbohydrate composition of juniper is clearly closer to the normal wood than the compression wood of spruce. In particular, the low amount of galactose indicates that the juniper sample would be normal wood. Galactose is abundantly present in compression wood as (1-4)-β-galactan (Mast et al., 2009, Timell, 1986), which is proposed to be concentrated in $S2_L$ layer (Altaner et al., 2010), a layer with high concentration of lignin within the S2 cell wall. The $S2_L$ layer is one of the most common features of compression wood (Gierlinger et al., 2010, Cóte et al., 1968, Donaldson et al., 1999, Wardrop, 1964, Fergus et al., 1969).

Table 6. Carbohydrate composition (% of neutral sugars) of spruce normal wood, spruce compression wood and juniper. (Paper III)

	Arabinose	Rhamnose	Galactose	Glucose	Xylose	Mannose
Spruce normal wood	1.3	0.3	5.5	67.7	9.0	16.3
Spruce compression wood	1.1	0.4	17.5	59.5	10.4	11.2
Juniper	1.4	0.5	7.4	61.9	11.9	17.1

Table 7. Lignin and extractives contents (% on dry wood) of spruce normal wood, spruce compression wood and juniper. (Paper III)

	Acid soluble lignin	Klason lignin	Extractives
Spruce normal wood	0.5	29.2	0.9
Spruce compression wood	0.5	37.2	1.7
Juniper	0.7	32.0	5.8

The distribution of lignin and cellulose within the cell wall can be analysed with Raman imaging without using any chemical treatments or staining of the sample. This way the introduction of artefacts that may be caused by accessibility of the cell wall and reactions or staining of unwanted components can be avoided. Raman imaging could even be done

directly from freshly cut fibres, since water does not disturb the measurements like it does in IR spectroscopy (Smith and Dent, 2005). However, the preparation of fresh samples has proven to be extremely difficult due to the sample surface smoothness requirements set by the confocal system. Raman spectroscopy and imaging is described in more detail in the Experimental section of this thesis.

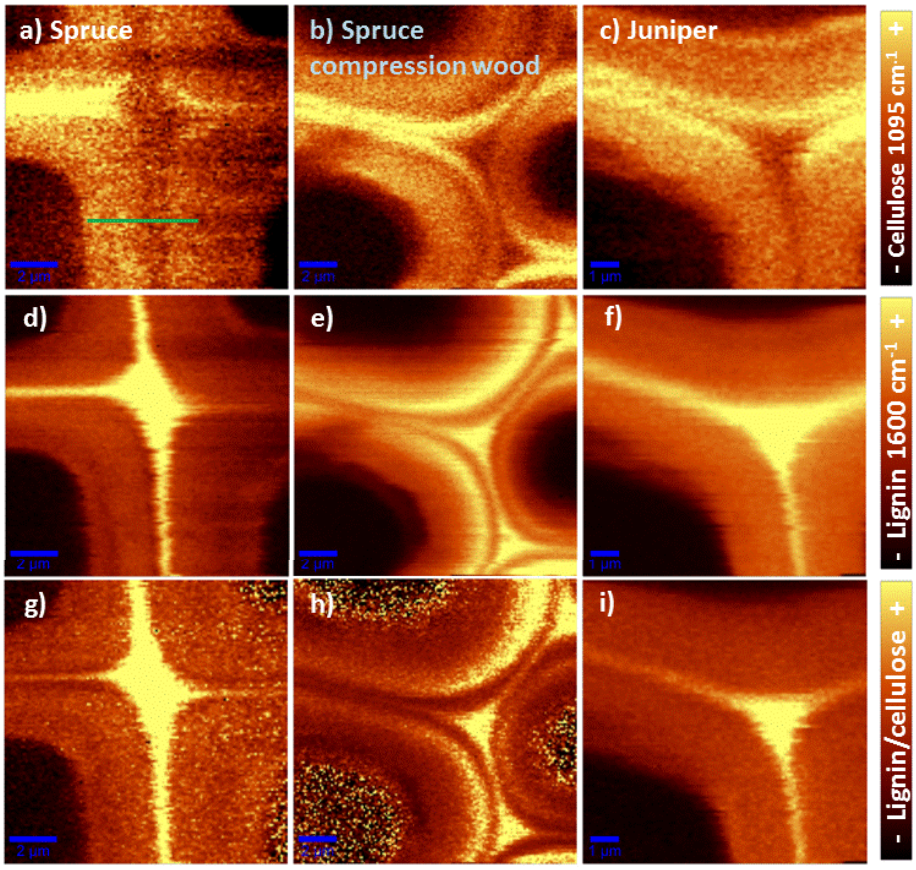

Figure 12. Raman images of spruce normal wood (a,d,g), spruce compression wood (b,e,h) and juniper (c,f,i). Images are constructed according to characteristic Raman band regions of cellulose (a-c) and lignin (d-f) as well as lignin/cellulose ratio (g-i). Raman band regions used are presented in Table 13. (Paper III)

The lignin/cellulose distribution in juniper resembles that of normal wood of any wood species analysed so far by Raman imaging (Gierlinger et al., 2010, Gierlinger and Schwanninger, 2006, Agarwal, 2006, Schmidt et al., 2009). The lignin/cellulose distribution throughout the secondary cell wall was even while the relative amount of lignin was drastically higher in primary cell wall and middle lamella. A similar distribution has also been observed with other techniques (Wardrop, 1964, Cóte et al., 1968, Fergus et al., 1969). Compression wood samples are easily distinguished by the high lignin concentration of the $S2_L$ layer, which is clearly visible in the images (Figure 12 e and h). A similar distribution has earlier been measured by Raman imaging from spruce compression wood (Gierlinger et al., 2010).

As seen in the Figures 12 and 13, all of the lignin/cellulose ratio distributions are very much alike. Practically no differences can be seen between juniper, spruce and pine, or even between hardwoods and softwoods. Similar results have also been reported in the literature (Agarwal, 2006, Gierlinger et al., 2010, Gierlinger and Schwanninger, 2006, Schmidt et al., 2009). Only cells from reaction wood or from genetically modified trees have been shown to differ in their lignin/cellulose distributions (Gierlinger et al., 2010, Schmidt et al., 2009).

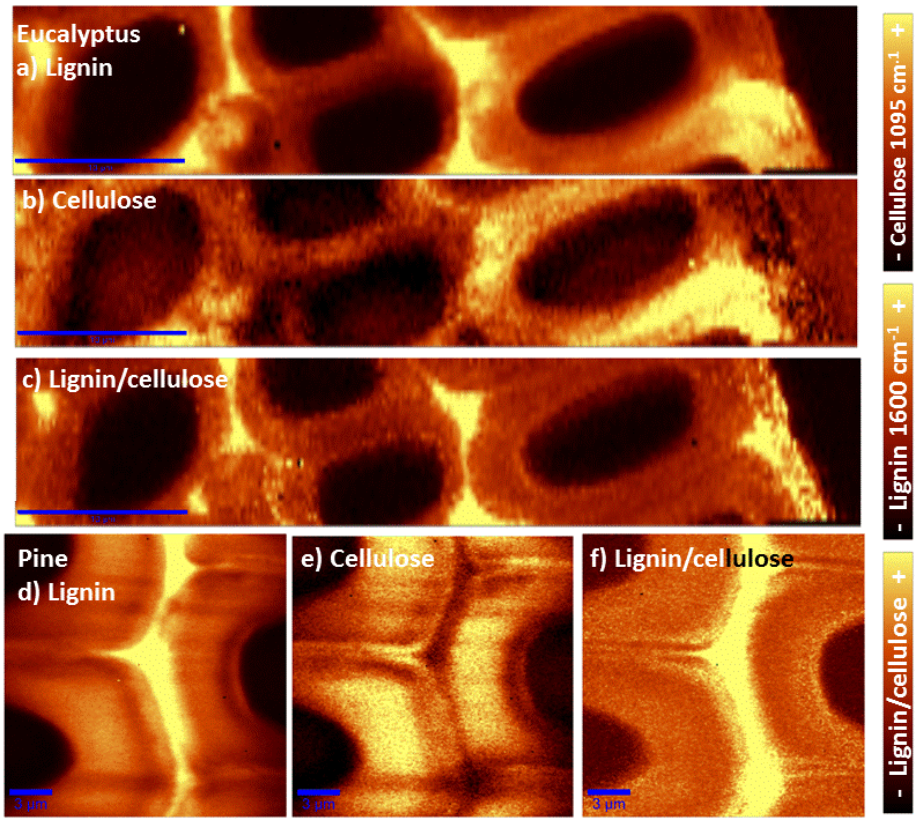

Figure 13. Raman images of eucalyptus (a-c) and pine (d-f). Images are constructed according to characteristic Raman band regions of lignin (a,d) and cellulose (b, e,) as well as lignin/cellulose ratio (c,f). Raman band regions used are presented in Table 13. (Paper IV and unpublished data)

This shows that although the appearance of trees may differ a lot from each other, they are basically constructed in the same way. The hierarchical structure of wood has been developed during millions of years to the way it is today and it is altered only under the severe circumstances. The wood is the only natural fibre composite, or nanocomposite, that has been used successfully by humankind in load bearing structural applications.

5.2 Analysis of juniper pulp

Juniper fibres were separated using conventional kraft pulping. The pulp was subsequently analysed with FibreLab and laboratory handsheets were prepared from it to determine the strength properties. Kraft pulping has been studied for over a century and handsheet testing is very well standardized, which makes them a viable way to analyse fibre properties. The fibre and handsheet properties of juniper were be compared to values obtained from literature (Table 8 and Table 10).

The kappa number of juniper pulp was much higher (56.4) than in commercial softwood kraft pulps (about 15-30) (Sjöholm et al., 2000, Kontturi and Vuorinen, 2006, Robertsen and Joutsimo, 2005, Joutsimo and Robertsen, 2004). This was considered to be caused by the high amount of branches in the juniper wood discs used for pulping. Branches are more difficult to pulp and they might remain relatively uncooked and a high lignin content in the pulp, which increases the Kappa number significantly. Since the aim of pulping was to analyse fibre properties, pulping parameters were not fine-tuned.

As can be seen from Table 5, the crystal width increases due to kraft pulping and the crystal length decreases. It has been considered that the increase of the crystal width is caused by the crystallization of the surface and aggregation of the microfibrils during pulping (Leppänen et al., 2009). On the other hand it has been proposed that the decrease in crystal length is caused by depolymerization of cellulose (Leppänen et al., 2009), although this seems unlikely.

The carbohydrate composition of juniper pulp was fairly similar to softwood pulps (Table 8). The contents of non-cellulosic carbohydrates were close to literature values, although, more specifically they were close to the highest values. This agrees with the high non-cellulosic carbohydrate content of juniper wood (Table 6).

Table 8. Carbohydrate composition (% of neutral sugars) of juniper pulp. Values for softwood kraft pulp handsheets were obtained from literature(Rydholm, 1965, Sjöholm et al., 2000, Hult et al., 2001). (Paper IV)

	Juniper	Softwood pulp
Arabinose	0.4	0.1-1
Xylose	9.4	4.5-9.4
Mannose	6.9	5-6.9
Galactose	0.3	0-0.5
Glucose	83.1	83.6-90.3

Juniper's fibre properties are very much like those of softwood compression wood fibres when comparing the fibre properties of commercial softwood pulps (Table 9). Small fibre diameter, thick cell walls and short fibres are characteristics of compression wood (Timell, 1986). Small and thick walled cells explain the high density of compression wood and juniper (Table 4).

Table 9. Fibre properties of juniper pulp measured by FibreLab. Values for softwood pulp is collected from the literature (Sáren et al. 2001, Rydholm, 1965, Kibblewhite, 1999, Seth, 2006, Gurnagul et al., 1992). (Paper IV)

	Fiber diameter (µm)	Cell wall thickness (µm)	Mean length (mm)	Coarseness µg/m	Curl %
Juniper	21	3.9	0.83	97	21.5
Softwood	23-56	2.8-3.8	1.5-3.6	130-300	16.4-22.9

When analyzing the fibre properties using handsheet testing, it is important to remember that the paper composed of a random network of fibres and unlike in single fibre testing, the fibre-fibre interactions also play an important role. For example curl and coarseness of fibres affect paper properties. Values for curl and coarseness are very close to the values of commercial softwood pulp and their effect can be assumed to be minimal. One potential factor affecting handsheet properties is the surface chemistry of the fibers. Its influence was, however, considered insignificant, based on the finding of a studies by

Maximova et al. (2001) and Koljonen et al. (2004) where adsorbed lignin did not significantly affect the strength properties of the handsheets.

The strength properties of juniper handsheets were poor when compared to commercial softwood pulp handsheets. One of the reasons for the poor strength properties is possibly the short fibre length of juniper. Also the fibre strength naturally contributes to the strength properties of the handsheets. MFA has been shown to significantly affect fibre strength. As the MFA increases, fibre strength decreases. In low MFA fibres, the fibrils are able to bear the tensile load. As the MFA increases the inter-fibrillar or matrix-fibril shear load increases, causing the fibrils to debond more easily or for failure to take place through shear yielding of the matrix, which leads to the destruction of the cell wall hierarchy and thus failure of the fibre.

Table 10. Handsheet properties of juniper kraft pulp handsheets. Values for softwood kraft pulp handsheets were obtained from literature(Joutsimo and Robertsen, 2004, Kontturi and Vuorinen, 2006, Seth and Page, 1988, Seth, 2006, Rydholm, 1965). (Paper IV)

	Tens. strength (Nm/g)	Stretch (%)	Stiffness (kNm/g)	Tear Index (Nm/kg)	Density (kg/m^3)
Juniper kraft pulp	36.9	5.4	3.4	9.4	584
Softwood kraft pulp	120-36	3.3-2.7	9.6-7.5	13-30	

On the other hand, the stiffness of the juniper handsheet was significantly lower and the stretch was twice that reported for commercial softwood handsheets. The elastic properties of handsheets have been shown to correlate well with the elasticity of individual fibres (Page and Seth, 1980).

Also stretch (strain to fracture) values of juniper handsheets were much higher than ones of softwood pulp handsheets. Elastic fibres with high MFA are able to deform before the bonds between the fibres or the fibres themselves start breaking, which results in high stretch values (Page and Seth, 1980).

The elastic properties of juniper wood do indeed manifest themselves in the properties of handsheet made from juniper pulp. The properties of randomly oriented fibre networks of paper correlate well with the properties of the solid wood (Table 4 and Table 10). Altogether the study on the juniper has shown that the chemistry of the fibres clearly does not contribute as much to the properties of the material as the cell wall hierarchy, especially MFA.

6. Effects of lignin composition on processibility of fibres

6.1 Differences in lignin functional group distribution in spruce and pine

The composition of lignin is known to vary significantly between different plants, and even between wood species (Sjöström, 1993). Some studies have also pointed out variations in lignin structures within a single wood cell (Whiting and Goring, 1982). The structure of lignin has been shown to have an effect in different industrial processes. One example of these is coniferyl aldehyde (CAld), the presence of which in lignin has been shown to affect the pulping of wood (MacKay et al., 1999). Although methods to analyze CAld are well known, there is a very little data on it (Adler et al., 1948).

CAld is considered to be an intermediate in the biosynthesis of coniferyl alcohol (CAlc). The amount of CAld groups in transgenic trees has been controlled by suppressing the activity of coniferaldehyde dehydrogenase (CAD), which is considered to be responsible for the reduction of CAld into CAlc (Boerjan et al., 2003).

Raman imaging was used to analyse the differences in lignin structures in spruce and pine. Raman bands characteristic to CAlc and CAld groups were chosen according to a study on ethylenic compounds in TMP by Agarwal and Ralph (2008). For Raman imaging, the characteristic Raman bands for CAlc and CAld groups were compared to the intensity of the 1600 cm^{-1} band which represents aromatic ring mode of lignin, since images constructed using only the characteristic bands yielded images that resemble each other exactly. All the wavenumbers used for imaging are presented in Table 13 in the Experimental section of this thesis.

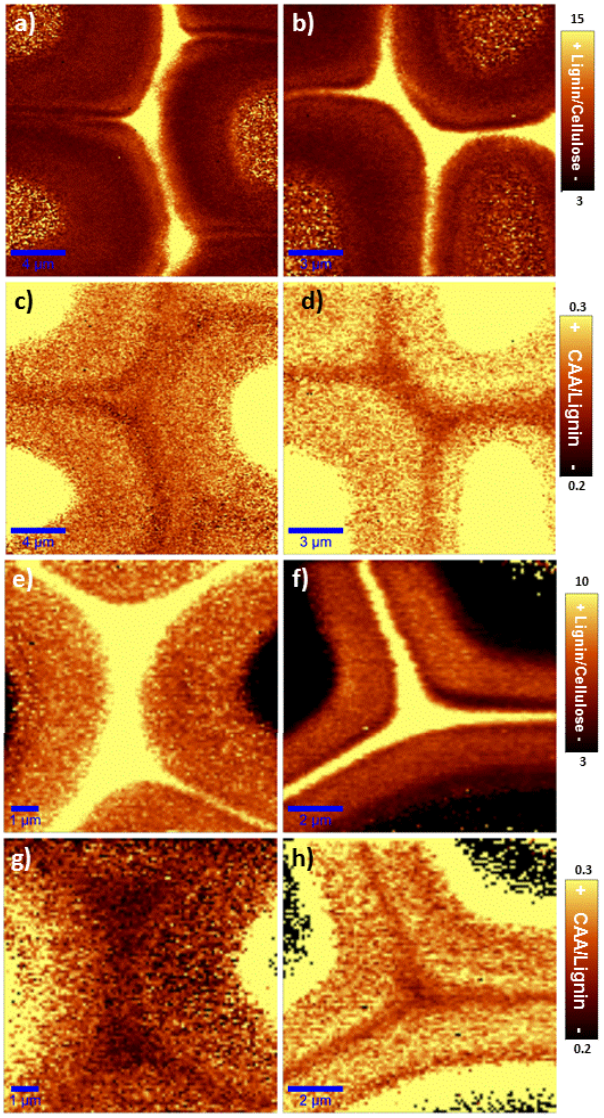

Figure 14. Raman images of pine (on left) and spruce (on right) samples before (a-d) and after (e-h) NABH4 treatment. Images are constructed according to lignin/cellulose (a,b,e,f) and CAA/lignin (c,d,g,h) Raman band ratios. Raman band regions used are presented in Table 13. (Paper V)

The Raman images constructed according to the ratio between bands representing both CAlc and CAld (joint abbreviation CAA for both structures) and lignin revealed clear differences between spruce and pine (Figure 14). In spruce, the CAA group content of lignin is higher in the secondary cell wall and decreases in the primary cell wall and middle lamella lignin. However, in pine, the CAA content in the vicinity of primary cell wall lignin was clearly lower than in middle lamella lignin and secondary wall lignin.

Since differences could only be seen from the images constructed according to the Raman band where both CAlc and CAld groups contributed, samples were treated so that a contribution from only one of the groups was present. $NaHB_4$ was used to reduce CAld groups to CAlc groups according to the method introduced by Agarwal and Ralph (2008). The reaction scheme of $NaHB_4$ reduction is presented in Figure 15. After reduction the differences between pine and spruce disappeared, and the CAA distribution in both species resembled that of unmodified spruce (Figures 14 c,d,g and h), where only two separate regions with differing CAA content can be observed.

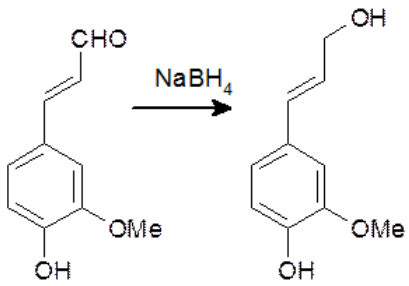

Figure 15. Reaction scheme for reduction of coniferyl aldehyde to coniferyl alcohol by $NaBH_4$.

Phloroglucinol staining is a well-known method for analysing CAld groups (Adler et al., 1948). However, studies on CAld groups have been scarce. A high concentration of CAld groups has been shown to be present in the region of a primary cell wall and S1 (Peng and Westermark, 1997). CAld distribution was studied by UV-Vis microscopy, which gives only the absolute number of groups, while in our study CAld content was reported as a ratio to the lignin content.

Although the difference in the distribution of one functional group of one cell wall component seems insignificant, it could have a large impact in certain industrial processes. One of such process is thermomechanical pulping, where the difference in the quality of pulp and the energy consumption of the process varies greatly between spruce and pine. In order to produce equally good TMP pulp from pine of equivalent quality to that of spruce, a much greater energy input is needed (Reme and Helle, 2001). The pulps from spruce and pine also differ in their surface chemical composition (Karnis, 1994).

It has been shown that the cleavage of fibres takes place in different parts of the cell wall in spruce and pine during TMP pulping. In spruce, the crack usually propagates at the interface between the primary and secondary cell wall, leaving the low lignin content secondary cell wall as the fibre surface. In pine, the crack propagates at the interface between primary cell wall and middle lamella, and between secondary cell wall and primary cell wall. This can result in fibres with a surface consisting of either low lignin content secondary cell wall, or primary cell wall with high lignin content (Fernando and Daniel, 2008).

Differences in the distribution of CAA groups in lignin could be used to explain differences in the processibility of pine and spruce. A high amount of CAld groups could indicate that lignin biosynthesis in the cell wall has been interrupted, which causes the lignin to have a lower molecular weight than it would normally have. Aldehyde groups are also hydrophilic groups and their increased amount could also increase the water content of the cell wall. Both decreased molecular weight and increased water content affect the glass transition temperature of lignin (Olsson and Salmén, 1997), which plays an important role in thermomechanical pulping (Irvine, 1985).

The cracks in the material form preferentially in the interphase of two different materials, as in this case lignins with differing amounts of CAld groups. In the case of spruce the only interphase of two different lignin types is in the region of the primary cell wall,

where the cracks have been shown by Fernando and Daniel (2008) to propagate during the TMP process. In pine, however, there are two interphases where lignin structure changes; between the secondary and primary cell wall regions and between the primary cell wall region and the middle lamella. These interphases correspond well to the defibration mechanisms of pine and spruce shown by Fernando and Daniel (2008).

6.2 SEC analysis of residual TMP lignin

Some middle lamella and primary cell wall particles consisting mainly of lignin remain on the surface of the TMP fibres (Li et al., 2006). The surface lignin was isolated from spruce and pine TMP pulps by extraction with 1,4-dioxane for further analysis to correlate the findings from Raman imaging with other analytical methods. Acetone extraction was performed prior to the dioxane treatment in order to remove extractives. 1,4-Dioxane is a well-known lignin solvent and its used, for example, in the isolation of milled wood lignin (Björkman, 1956), which is maybe the most popular model compound for native lignin (Guerra et al., 2006). 1,4-Dioxane does not dissolve the cell wall polysaccharides and thus it extracts only the lignin from the surface of the fibres. The lignin inside the cell wall remains sterically locked in the hemicellulose matrix. As can be seen from the scanning electron microscope (SEM) images of TMP fibres more fibrillar structures, which most likely are bundles of cellulose microfibrils, are revealed after extraction with acetone and 1,4-dioxane (Figure 16). This suggests that the covering layer of lignin is removed due to extraction.

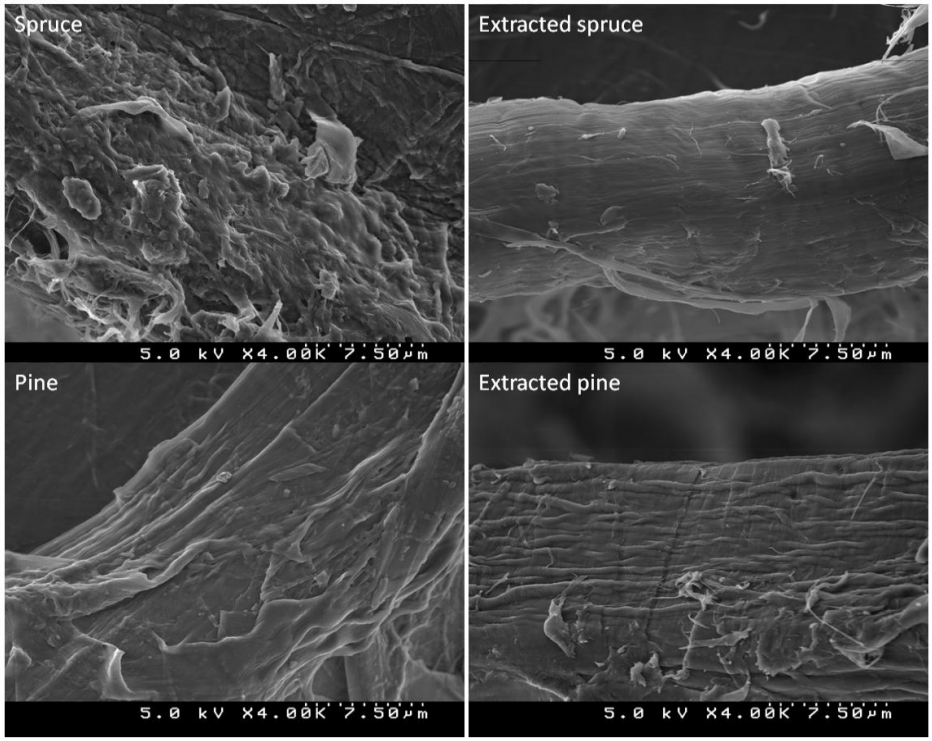

Figure 16. SEM micrographs of unextracted and extracted spruce and pine TMP fibres. (Unpublished data)

Removal of residual lignin seen in the SEM images was further supported by ESCA measurements. ESCA is a sensitive method to analyse only the very surface of the samples (Johansson, 2002), and thus it can be used to analyse changes on the surface of the fibre. The O/C ratio and CC-carbon values of the samples were used to analyse the chemical composition of the fibre surfaces. The O/C vs. C-C graph shows that the composition of unextracted sample surfaces are close to lignin and extractives, while the extracted ones are closer to cellulose (Figure 17). No significant differences, however, could be observed between the acetone extracted fibres and the ones further extracted with 1,4-dioxane. This indicates that the changes due to dioxane extraction subsequent to acetone extraction cause only minor alterations in the surface chemistry of the fibres and they cannot be observed with ESCA

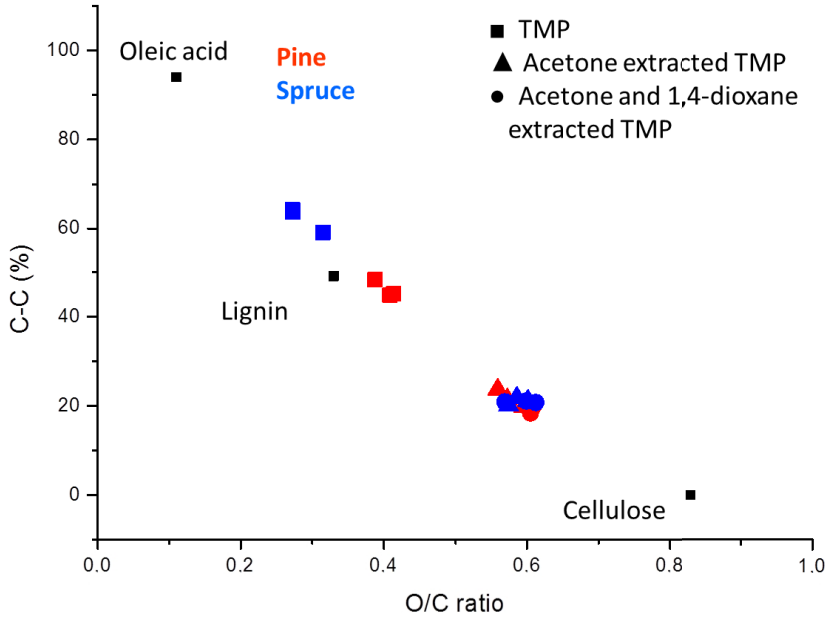

Figure 17. O/C vs. C-C graphs. Values for cellulose, lignin and oleic acid (*) are calculated from their chemical compositions. (Unpublished data)

The dioxane was evaporated and the extract dissolved in LiCl/DMI. LiCl/DMI was chosen as a solvent for the lignin extract because studies have shown that softwood pulps dissolve better in it. A similar study exists where residual lignin from kraft pulp was dissolved with LiCl/DMAc and analysed by using size exclusion chromatography (SEC) (Sjöholm et al., 1999).

The UV and differential refractive index (RI) chromatograms from SEC measurements are presented in Figure 18. From the RI chromatogram we can see that there is no difference in the shape of the peak between the samples. The data from the UV detector, operating at 244 nm wavelength, show a difference between spruce and pine samples. In pine there is a visible shoulder in the chromatogram, while the shape of the spruce peak is much more uniform. The difference could indicate that the residual lignin in pine

consists of two fractions with distinct molecular weights while the composition of spruce lignin is much more uniform.

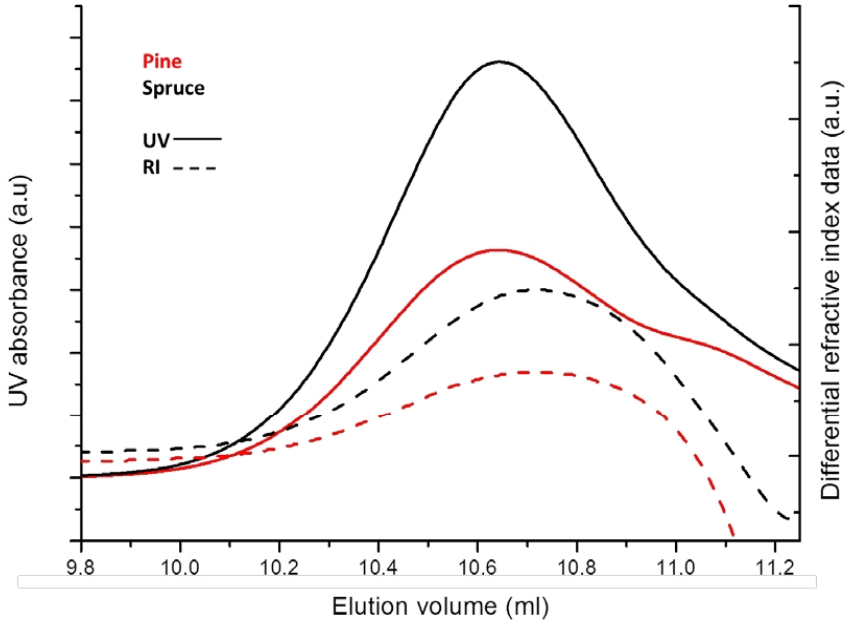

Figure 18. RI and UV chromatograms of 1,4-dioxane extracts from spruce and pine. (Unpublished data)

This finding correlates with the Raman imaging results on the CAA distribution in spruce and pine. The residual lignin extracted from the surface of the pine TMP fibres consists of two molecular weight fractions, which were detected in the SEC-UV chromatogram. The lower molecular weight lignin fraction possibly contains the primary cell wall lignin with a high CAld concentration. Since the CAld groups remain in lignin due to the interrupted biosynthesis, the molecular weight of such lignin can be assumed to be lower. Two fractions of pine lignin in the primary cell wall and the middle lamella lignin can also be seen in the Raman images in Figure 14. The uniform peak of dioxane extract from spruce indicates that the lignin in the primary cell wall and middle lamella is more homogeneous.

6.3 SEC analysis of residual lignin in oxygen delignified birch and eucalyptus kraft pulps

A vast quantity of chemicals is needed to remove the lignin from wood fibres in the production of bleached pulp for paper making. The most common delignification process subsequent to pulping is oxygen delignification. Oxygen delignification removes about 50 % of the residual lignin from kraft pulp. The bleaching sequence, i.e., further removal of residual lignin after oxygen delignification is dependent on the raw material used for pulping.

Lignin-carbohydrate complexes (LCCs) are known to play an important role in the removal of the residual lignin. LCCs are known to be formed during alkaline pulping. However, they are assumed to be also present in native wood. LCCs have been considered to be one of the main reasons for difficulties in removal of the residual lignin from pulps. In order to avoid harsh bleaching sequences that damage fibre properties and increase the consumption of chemicals, and understanding of the ultrastructure of different materials for pulping is necessary.

Oxygen delignified birch and eucalyptus kraft pulps were analysed by SEC with multi-angle laser light scattering (MALS), RI and UV system using LiCl/DMAc as solvent. As can be seen in Table 11, the pulps were fairly similar to each other. The birch pulp had a slightly higher content of xylose and a lower content of glucose than the eucalyptus pulp. The viscosity and Kappa number of the birch pulp were slightly higher than those of the eucalyptus pulp.

Table 11. Carbohydrate composition, extractive content, kappa number and intrinsic viscosity of birch and eucalyptus pulps. (Paper VI)

	Arabinose (%)	Xylose (%)	Mannose (%)	Galactose (%)	Glucose (%)	Extractives (%)	Kappa Number	Intrinsic Viscosity (ml/g)
Eucalyptus	0.2	13.1	0.2	0.2	84.1	0.31	11.9	1057
Birch	0.2	21.8	0.4	0.0	73.8	0.21	13.2	1270

Dissolution of the sample can be evaluated from the slope of conformation plot, which is a log-log plot of radius of gyration versus molecular weight. If the solvent is good, the slope value falls between 0.5 and 0.6, which indicates random coil formation. Since the slopes of conformation plots (Table 12) fell between 0.5 and 0.6, the dissolution of the samples could be considered good. Eucalyptus and birch pulps yield very similar bimodal RI chromatograms (Figure 19), although the molecular weights and ratios of the two fractions differ slightly. The high molecular weight (HMW) fraction of birch pulp has a slightly higher average molecular weight than the eucalyptus pulp, whereas the average molecular weight of the low molecular weight (LMW) fraction was higher in eucalyptus. The higher molecular weight of HMW fraction in birch pulp indicates that the cellulose has a higher DP compared to eucalyptus pulp. The lower molecular weight of LMW fraction of birch pulp, in turn, denotes that hemicelluloses have a higher DP in eucalyptus pulp. It can also be seen from the fact that the average molecular weights of the samples are almost the same but the hemicellulose content of birch pulp is higher than in eucalyptus. The higher amount of hemicelluloses is also likely to be the reason for the higher polydispersity of the sample (Table 11).

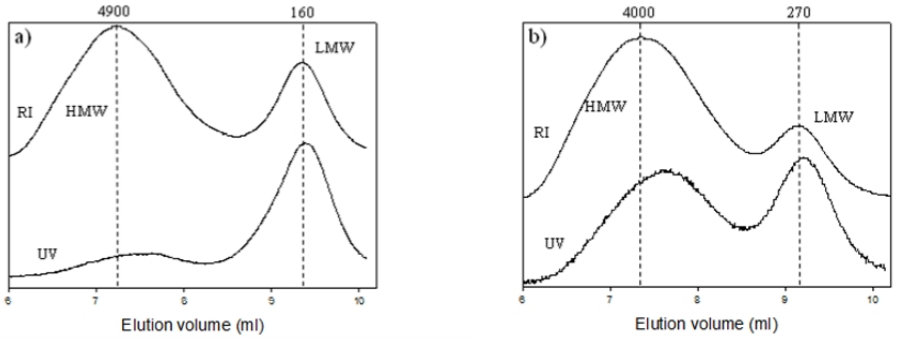

Figure 19. UV and RI chromatograms of oxygen delignified birch (a) and eucalyptus (b) kraft pulps. (Paper VI)

Although the RI choromatograms of birch and eucalyptus pulps resembled each other, there are significant differences in UV chromatograms. The HMW fraction of birch pulp has a very small UV light response whereas the LMW fraction is strongly UV light absorbing. In eucalyptus pulp the HMW UV absorption band is slightly larger than the one in the low molecular weight fraction (Table 12, Figure 19). This indicates that a large amount of the lignin in eucalyptus is associated with HMW fraction, which consists mainly of cellulose. This brings out the question of the lignin-cellulose association in pulps. Are there lignin-cellulose complexes present in pulp? And if so, how do their quantities vary in different kinds of pulps?

Table 12. Calculated parameters from SEC analysis of birch and eucalyptus pulps. (Paper VI)

	Slope of Conformation	Mw (kDa)	Mw/Mn	HMW RI Area/ Total RI Area	HMW UV Area/ Total UV Area
Eucalyptus	0.55	670	3.96	0.80	0.61
Birch	0.53	662	7.54	0.72	0.27

Although in many publications lignin has been proposed to be linked with cellulose (Lawoko et al., 2005, Isogai et al., 1989, Henriksson et al., 2007, Capanema et al., 2004), there has been debate whether cellulose-lignin LCCs exist (Kilpeläinen et al., 2007, Tenkanen et al., 1999). Li et al. (2011) recently analysed thioacidolysis products obtained from eucalyptus pulp and wood and found lignin-carbohydrates consisting of two different fractions, one rich with xylan and the other with glucan.

LCCs have been assumed to play an important role in the delignification of natural fibres and they have been even proposed to be the main reason for the difficulties in delignifying the pulp. In order to remove almost all the residual lignin from the pulp, it needs to go through several different bleaching sequences that damage the fibre and consume significant amounts of chemicals. Understanding how the lignin is associated with the other cell wall polymers will help us tailor the bleaching sequences for various materials and consume lesser amounts of chemicals.

7. Conclusions

The ultrastructure of fibres determines the properties of the material and how it reacts to different processes. This thesis covers a range of ultrastructural studies from naturally occurring deviations in chemistry or hierarchy of the cell wall to the effects of processing on the fibre properties.

The structural hierarchy of the cell wall was found to override the effects of differences in fibre chemistry on mechanical properties of both fibres and wood. Especially microfibril angle was found to determine the elasticity and tensile strength of natural fibre composites, in this case paper and wood. High microfibril angle fibres resisted tensile load poorly, which could be seen as very low tensile strength of handsheets and tensile failure as preferred failure mechanism of wood samples in 4 point bending tests. The low tensile strength could be explained by composite theory, where reinforcing fibres are more likely to debond from the surrounding matrix material as they become more aligned against the applied load. The elastic modulus of wood and stiffness of handsheets were very low in the case of high microfibril angle material, where reinforcing cellulose microfibrils have higher mobility inside the cell wall. Disruptions in the cell wall structure were observed to lower slightly the fibre tensile strength.

A more severe effect was observed in the susceptibility of the defected areas to acid hydrolysis. The degree of polymerization of fibres decreased more drastically in more defected fibres after acid hydrolysis than in ones with less structural defects.

The distribution of the cell wall structural components did not seem to have effect on the fibre properties. No differences could be seen in the lignin/cellulose distribution of any of the normal wood samples of different wood species from the “chemical micrographs” obtained by Raman imaging. This correlated well with measurements with other techniques in the literature. A different distribution of lignin and cellulose was only observed in compression wood.

Although no differences could be observed in the distributions of the cell wall structural components, spruce and pine differed in the distributions of lignin functional groups. The middle lamella and primary cell wall lignin in spruce appeared to be very homogeneous, while in pine they clearly consisted of two fractions with differing amounts of coniferyl aldehyde groups. Size exclusions chromatography measurements supported the Raman imaging findings on differences in lignin composition. Lignin with high coniferyl aldehyde group content is known to have a low molecular weight, which in turn could affect the physical properties of lignin in elevated temperatures so that it could possibly be used to explain the differences in the defibration behaviour of pine and spruce during thermomechanical pulping.

Differences in the ultrastructure of fibres could be also observed in processed fibres. A significant amount of lignin was found in SEC studies to be associated with the high molecular weight fraction of the oxygen delignified eucalyptus pulp sample, which is considered to consist mainly of cellulose. In birch pulp most of the lignin was associated with the low molecular weight fraction, corresponding to the hemicelluloses. There has been debate on the lignin-cellulose complexes, and these results point in favour of their existence. Differences in lignin-carbohydrate complexes might prove out to play a significant role in further delignification of the pulps.

The findings of this thesis bring out some implications of the complex nature of natural fibres. Instead of considering natural fibres merely as microscopic fibres, their nanocomposite structure has to be also acknowledged. The alignments of reinforcing fibres in walls of individual cells have a substantial effect on the properties of the whole plant. The plant cells have evolved to be “perfect” natural fibre composites in ambient conditions where the subtle differences in chemical composition do not play an important role. However, when the conditions are changed drastically, the effects of chemical differences become more prominent and differences between different species become significant.

Understanding the composite structure of natural fibres and their function in plants will give us valuable information on the behaviour of nanocomposites and provide us with model that can be used to design man-made composites. Knowledge on even the slightest details of fibres might aid us to develop processes to enhance fibre utilization.

8. Materials and Methods

8.1 Materials

Flax fibres were provided by Ekotex, Namysłów, Poland. The flax samples were supplied as green stem (i.e. before retting), as retted stem and as two fibre grades, "noils" and "kotonina" (Table 1). Noils are flax fibres mechanically separated from the stem and cleaned of shive. Additional mechanical processing of the noils, separating the fibres further, yields kotonina. The hemp fibre was mechanically separated from the stem and had the shive removed (in processes known as 'scutching' and 'carding' respectively), but had not undergone any further processing.

Hemp fibres were provided by BaFa GmbH, Malsch, Germany. To investigate whether increasing levels of damage induced by a particular mechanical process affected the susceptibility of hemp fibre to chemical degradation, a series of fibres that had been artificially damaged were prepared. Hemp fibres were passed a varying number of times through intermeshing cogwheels and the damage to the fibres was reported as the number of passes (0, 5, 12 and 22) the fibres made through the equipment.

Pine and spruce samples used in the determination of the CAA group distributions by Raman imaging were provided by KCL (Espoo, Finland).

Birch and eucalyptus samples were provided by Stora Enso, Imatra, Finland.

Stems of common juniper (Juniperus communis L.) were collected from Solböle, South-Western Finland. Samples were cut from the same, approximately 7 cm thick, straight and branchless stem roughly at a height of 50 cm.

Norway spruce compression wood and normal wood samples for 4-point bending tests were obtained from Mikkeli, South-Eastern Finland. Branchless samples were cut from

the same stem; normal wood being taken from approximately breast height and compression wood lower in the stem, close to the stump.

Oxygen delignified kraft birch and eucalyptus kraft pulps were provided by Finnish pulp mills.

8.2 Mechanical testing

Juniper, spruce and spruce compression wood were cut into small rectangular beams with dimensions 3 mm (radial), 6 mm (tangential) and 60 mm (longitudinal). Specimens were conditioned in a climate chamber (RH 65 % and 20 °C) prior to testing.

Annual ring width in juniper is smaller than in spruce and spruce compression wood, which results in a different number of annual rings in the sample. Therefore there is a variance in late wood percentage in the sample cross-section, which may slightly affect the modulus of elasticity.

A four point bending test with an outer span of 37.5 mm and an inner span 12.5 mm was used to determine mechanical properties (Figure 20). Testing was performed using a small, stepper motor driven, loading device designed for the use with a light microscope. Force was measured with a 500 N load cell. The loading was conducted under displacement control at a cross-head displacement rate of 0.5 mm/min. Specimens were loaded to 50 N and then unloaded to 5 N prior to the actual measurement, whereafter the samples were loaded to failure.

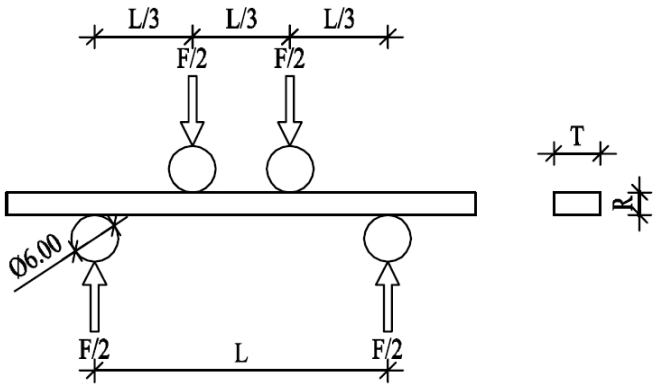

Figure 20. The 4-point bend test set-up; L is outer span, L/3 is inner span, R is specimen height and T is specimen width.

During testing, load and crosshead displacement data were recorded and bending behaviour was observed using an optical microscope equipped with a CCD camera. Micrographs were captured at 5 N loading force intervals.

The longitudinal modulus of elasticity was calculated from the classical formula of beam theory for homogenous beams with rectangular cross section. Total cross-sectional area was used. The modulus of elasticity was calculated based on crosshead displacement (which equals deflection of a beam under loading head) and load data between 0.1 and 0.4 of the maximum load. The effect of shear force and the indentation of the supports and loading head were neglected.

Equation 1

$$MOE_B = \frac{5}{27} \cdot \frac{L^3}{T \cdot R^3} \cdot \frac{\Delta F}{\Delta f}$$

where MOE_B is MOE determined in 4-point bending, L is outer span, T is specimen width, R is specimen height, ΔF is load difference and Δf is deflection under the loading head (Gere, 1997).

8.2 Single fibre testing

Single fibres were isolated for mechanical testing by soaking technical fibres (fibre bundles) in tap water and manually separating the ultimate fibres (individual cells) by using tweezers. The single fibre tensile testing was performed according to an adaptation of the ASTM D3379-75 (1989) standard. After drying, individual fibres were glued across a 10 mm aperture (gauge length) punched into card holders, using PVA adhesive.

Mechanical testing was carried out on a TSL 400 tensile testing machine (MTS, USA, www.mts.com) equipped with a 50 N load cell. Fibres were tested to failure at a rate of 0.5 mm/min. Twenty (20) fibres were tested from each fibre type. Before tensile testing, the cross-sectional dimensions of each fibre were measured from 3 locations along the gauge length using an optical microscope. The average value of the three measurements was used in the calculation of tensile stress. A circular cross-section was assumed. As no direct measurement of strain was possible, fibre strain was calculated from the crosshead displacement and is therefore likely to underestimate the true modulus due to the compliance of the system and other errors. Tests were deemed invalid if the fibres did not fail within the gauge length.

8.3 X-ray diffraction measurements

X-ray diffraction (XRD) measurements were conducted for solid pieces of juniper and for the compression and normal wood of Norway spruce. All the samples were cut tangentially from the stems using a scalpel to a (radial) thickness of about 1 mm (the longitudinal and tangential dimensions being about 10 x 10 mm^2). Two samples were cut from the juniper stem at the middle between the pith and bark; being 1 mm thick, the pieces included several annual rings. The spruce normal wood samples were cut from the earlywood of the 16^{th} and the 19^{th} annual rings, and the compression wood samples were from the earlywood of the 20^{th}, the 21^{st} and the 22^{nd} annual rings.

The MFAs were determined for juniper wood from the azimuthal intensity profiles of the cellulose reflection 004 measured using the symmetrical transmission geometry. The MFA distributions were determined from the azimuthal intensity profiles of the cellulose reflections *200* and *004* measured in symmetrical transmission mode using a set-up consisting of a Huber 420/511 four-circle goniometer, a sealed Cu-anode x-ray tube, and a NaI(Tl) scintillation counter. $CuK\alpha_1$ radiation (wavelength 1.541 Å) was obtained using a ground and bent germanium monochromator. The MFAs were determined from the intensity profiles by fitting pairs of Gaussian functions into the profiles as explained in (Sáren et al., 2001).

Diffraction patterns were measured using the same x-ray set-up for determining the dimensions of cellulose crystallites. The crystal length was determined from the reflection *004* measured in symmetrical transmission mode, and the crystal width was determined from the reflection *200* measured in symmetrical reflection mode. The crystal dimensions were obtained from the widths and positions of the reflections by the Scherrer equation (Andersson et al., 2000).

8.4 Scanning electron microscopy

Spruce and pine TMP fibres were sputter with ca. 2.5 nm thick osmium-coating layer at 7 Pa and 10 mA for 5 sec (Neo Osmium Coater, Meiwafosis, Japan). The samples were analysed with a field-emission-type SEM (Hitachi S-4000, Hitachi, Japan) at 5 kV.

8.5 Viscosity measurements

Viscosity measurements are among the most common chemical analyses made for pulp. In the standard method (SCAN-CM 15:99), the sample is dissolved in cupriethylenediamine (CED) and the efflux time at 25 ^{o}C of the solution is determined with capillary viscometer (Figure 21). The intrinsic viscosity is calculated from the

concentration and the efflux time of the solutions by first determining the viscosity ratio η_{ratio} with equation

Equation 2

$$\eta_{ratio}=ht$$

where h is the calibration constant for the viscometer and t is the efflux time for the test solution. The viscosity ratio is used to obtain a value for the product $[\eta]c$ from the table provided in the standard. The intrinsic viscosity $[\eta]$ is calculated from equation

Equation 3

$$[\eta]=[\eta]c/c$$

where c is the concentration of the test solution.

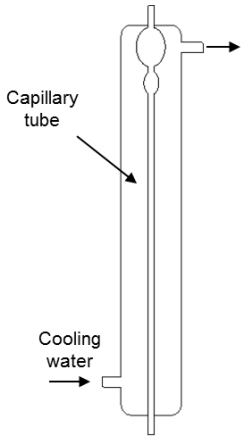

Figure 21. Capillary viscometer

The intrinsic viscosity of the polymer solution has been shown to correlate with the DP of the polymers following to Mark-Houwink-Sakurada equation:

Equation 4.

$$[\eta]=K_m M^{\alpha}$$

where M is the molecular weight and K_m and α are constants that can be found in the literature (da Silva Perez and van Heiningen, 2002). Evan and Wallis (1989), however, have shown that the Mark-Houwink-Sakurada equation underestimates the actual DP of cellulose. Intrinsic viscosity values can be used to correlate with the average DP, meaning that non-cellulosic cell wall components also contribute to the value.

Da Silva Perez and van Heiningen (2002) have recently developed an equation that can be used to determine the DP of cellulose and hemicelluloses from the intrinsic viscosity value when the carbohydrate content of the material is known.

8.6 Raman spectroscopy

The Raman effect was discovered by Krishna and Raman in 1928. However, before the introduction of FT-Raman in 1986 there are only a few reports where Raman spectroscopy has been applied to chemical analysis (McCreery, 2000). Among the reasons for this were technical difficulties and the subsequent, somewhat suppressed utilization of Raman spectroscopy, are the weak intensity of Raman scattering, fluorescence interference, and the inefficiency of light collection and detection.

Raman spectroscopy is based on detection of scattered photons after the excitation of a sample by monochromatic light. The basic principles of spectroscopic transition phenomena concerning Raman spectroscopy are illustrated in Figure 22. The sample is excited with monochromatic light (hv_0) to a short-lived "virtual state". Predominantly the molecules relax to the same ground state (v_0), scattering the photons of the same energy as used for excitation. This phenomenon is called Rayleigh scattering, which is a competing effect to Raman scattering. With a small probability the molecule relaxes to a

higher ground state (v_1), which results to an inelastically scattered photon with lower energy than the excitation energy. This is called Stokes scattering and it is the main phenomenon in Raman spectroscopy. Some of the scattered photons can also have an increased energy, which is called anti-Stokes scattering.

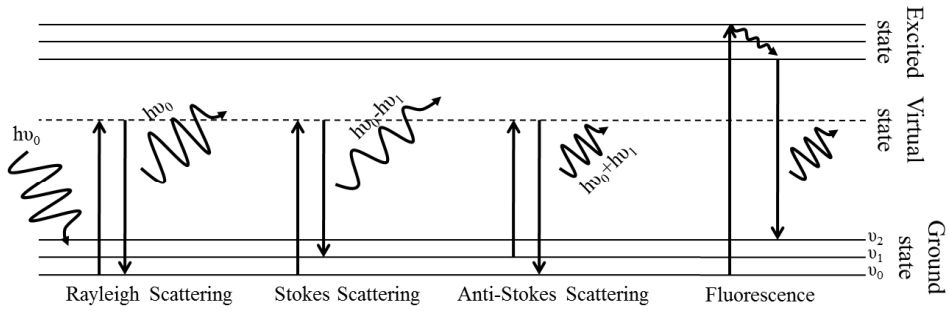

Figure 22. Spectroscopic transitions related to Raman spectroscopy.

Raman spectroscopy operates by the same energy range as IR spectroscopy and the chemical information yielded by the techniques are complementary. IR spectroscopy detects changes in the dipole moment, whereas Raman spectroscopy detects changes in polarizability. Symmetrical changes cause large polarization changes and hence strong Raman scattering and weak or no IR absorption, while the deformation mode causes weak Raman scattering and strong IR absorption (Figure 23). As a rule of thumb what can be seen in Raman spectroscopy is not visible in IR and vice versa (Smith and Dent, 2005).

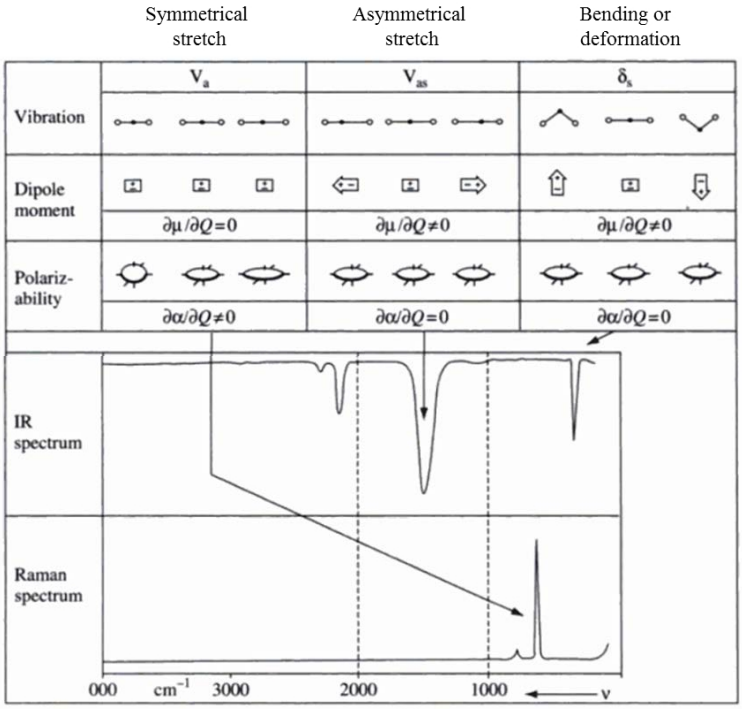

Figure 23. Dipole and polarization changes in carbon disulphide with resultant IR and Raman spectra (Smith and Dent, 2005)

When it comes to biological hydrophilic samples, such as natural fibres, the insensitivity to very polar water can be considered to be an advantage of Raman spectroscopy. This also enables measurements directly from water solutions.

Although Raman scattering was discovered with the naked eye, the phenomenon is inherently very weak. Only 10^{-6}-10^{-8} of photons are Raman scattered, which has set high requirements on the detection equipment. Due to the weak nature of Raman scattering, high energy lasers are needed, which in turn easily result in degradation of the sample (Smith and Dent, 2005). Weak Raman scattering can also be easily suppressed by fluorescence. Fluorescence can originate from the impurities in sample or from the

sample itself. For example, degradation products of lignin usually fluoresce so strongly that no Raman bands from the sample itself can be distinguished.

8.7 Raman imaging

Raman imaging can be thought of as "chemical microscopy". The principle of Raman imaging is presented in

Figure **24**. First an area of interest is located using an optical microscope. After the area is chosen, Raman spectra are collected within the area at regular intervals. Subsequently the baselines of the spectra are corrected and characteristic bands representing the features of interests are chosen. Raman images are constructed from the corrected spectra according to the intensity or intensity area of the selected Raman bands.

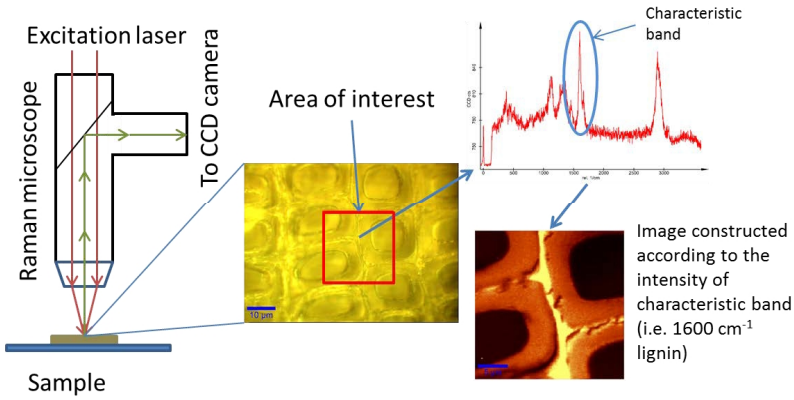

Figure 24. Schematic image of Raman microscope and the basic principle of Raman imaging.

Raman imaging sets very high requirements for the samples. To obtain high resolution images, a confocal microscope with high magnification is needed. When measuring large areas, the sample needs to stay in the focus of the microscope during the entire measurement. For example, when preparing wood cross-sections for Raman imaging, the sample needs to be embedded and sectioned with a microtome in order to achieve surfaces that are smooth enough.

Raman images may consist of tens a thousands of spectra, which means that the measurements are very long and the sample needs to endure a high powered laser for the whole measurement. When constructing a Raman image, usually compromises are made between the resolution of the image and the quality of the spectrum. With an increasing amount of measurements, however, the features of the images will be clearer and the quality of the spectra will be lower due to shorter measurement time or a lower laser intensity in order not to burn the sample during the measurement.

Raman spectroscopy and imaging in natural fibre research

Raman spectroscopy has been proven to be a powerful tool in analysis of different components of cell wall. Various features of cellulose have been analysed by Raman spectroscopy, for example crystallinity (Agarwal et al., 2010, Schenzel et al., 2005), different polymorphs (Atalla, 1976, Wiley and Atalla, 1987, Schenzel and Fischer, 2001), orientation (Atalla et al., 1980) and strain (Eichhorn et al., 2000, Eichhorn and Young, 2001). Strain measuments have been applied for pure cellulose fibres (Eichhorn et al., 2003), but also for flax, hemp (Eichhorn et al., 2000) and wood fibres (Gierlinger et al., 2006). The spectrum of cellulose is, like the spectrum of any polymer (Tanaka and Young, 2006), sensitive to orientation when using polarized light in analysis (Wiley and Atalla, 1987).

Non-cellulosic polysaccharides such as pectins and hemicelluloses in the wood cell wall have also been under investigation. However, due to the overlapping of their spectrum with all of the cell wall components, Raman imaging of hemicellulose and pectins has not been succesful so far (Atalla and Agarwal, 1986, Agarwal and Ralph, 1997).

Lignin is perhaps the easiest cell wall component to analyse due to very prominent bands arising from the aromatic ring structures at 1600 cm^{-1} wavenumber region. Raman spectroscopy has been used to show that lignin inside the cell wall has orientation with respect to cellulose (Atalla and Agarwal, 1985). Raman spectroscopy has also been used to analyse for example, guaiacyl/syringyl ratios (Takayama et al., 1997), carbonyl groups

(Kihara et al., 2002) and ethylenic compounds in lignin (Agarwal and Ralph, 2008) as well as lignin concentration in pulps (Agarwal et al., 2003). A significant advantage in lignin analysis can be gained when using UV-wavelength laser for the excitation of the sample. Raman bands of aromatic structures (about 1600 cm^{-1} wavenumber area) are resonance enhanced and more information can be extracted from the spectrum of lignin (Halttunen et al., 2001, Saariaho et al., 2005, Jääskeläinen et al., 2006). UV-resonance Raman spectroscopy can also be used to detect hexenuronic acid groups in pulps (Jääskeläinen et al., 2005).

Since the Raman instruments, for example computers and CCD cameras, have been only recently developed to such high level that enabled easy Raman imaging, there are relatively few publications involving this technique. Raman imaging has been used to analyse chemical distributions in conventional (Gierlinger and Schwanninger, 2006, Agarwal, 2006), as well as transgenically modified trees (Schmidt et al., 2009). The sensitivity of Raman spectroscopy to the orientation of cellulose has enabled detection of microfibril angle in different parts of the cell wall (Gierlinger et al., 2010, Agarwal and Ralph, 2007).

Equipment

The samples were analyzed with an alpha300 R Confocal Raman microscope (Witec GmbH, Germany, www.witec.de) at ambient conditions. The Raman spectra were obtained by using a frequency doubled Nd:YAG laser (532.35 nm, 10 mW) and a Nikon 100× (NA=0.95) air objective. The Raman system was equipped with a DU970N-BV EMCCD camera behind a 600 lines/mm grating. The excitation laser was polarized horizontally. For each single spectrum in the Raman images, an integration time of varied length was used depending on how prone the samples were to burn. The size of one pixel in the image is 0.1 µm. The baseline of the spectra were corrected with WiTec Project 1.94 (WiTec GmbH, Germany, www.witec.de) by using fifth order equation in the wavenumber area from 600 cm^{-1} to 2000 cm^{-1}, where the most prominent Raman bands are located. A constant background was not subtracted from the spectra due to the

varying baseline of the individual measurements. A list of characteristic wavenumber regions used for constructing images is presented in Table 13.

Table 13. Raman band regions of compounds for construction of images.

Compound	Wavenumber region (cm^{-1})	Raman mode
Lignin	1583-1620	Aromatic ring mode
Cellulose	1090-1100	C-O stretch
Epoxy resin	1726-1754	
Coniferaldehyde and alcohol (CAA)	1649-1677	C=C and C=O stretch
Coniferaldehyde	1623-1633	C=C stretch

8.8 Size exclusion chromatography

Size exclusion chromatography (SEC) is a liquid chromatographic separation method for macromolecules by their molecular size. Figure 25 illustrates the basic principle of SEC with macromolecules of two different sizes. As the macromolecules pass through the column packed with porous material with a controlled pore size, the small particles penetrate the pores, which cause them to retain longer in the column than the large particles that pass right through the column. A more detailed description on SEC can be found from Handbook of Size Exclusion Chromatography (Malawer and Senak, 2004)

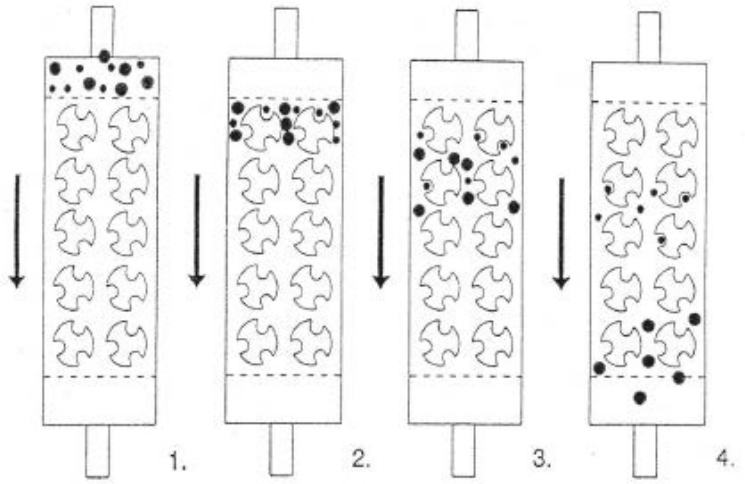

Figure 25. Basic principle of SEC (Malawer and Senak, 2004)

After the molecular weight fractions have passed through the column in reversed order so that the high molecular weight fraction elutes first, they can be analysed with different kinds of detectors. In this work MALS, RI and UV detectors were used.

The RI detector is the most common detector used in SEC systems. It detects very small changes in the refractive index of the solution and can be used to detect concentrations of most of the polymeric samples. The UV detector measures the absorption at a certain wavelength or a range of wavelengths. UV detectors can be used, for example, for samples containing aromatic or olefinic structures (Malawer and Senak, 2004).

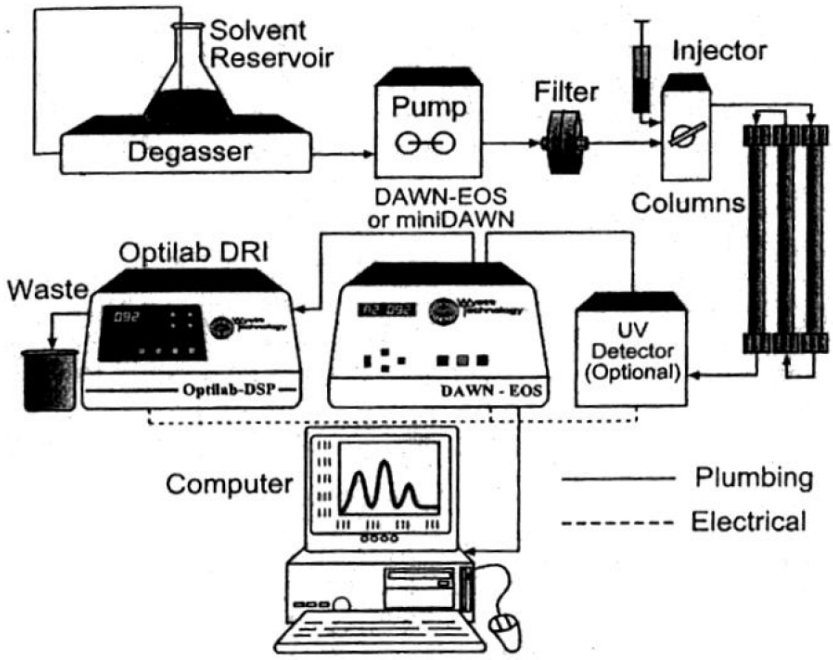

Figure 26. Schematic image of a SEC system (Malawer and Senak, 2004) .

The intensity of the light scattered from a polymer solution, in addition to that scattered by pure solvent, is related to the molecular weight and the shape of the polymer in solvent. The shape and the polymer size are determined from the angular variations of the scattered light intensity. The weight-average molecular weight, the radius of gyration and the second virial coefficient can be determined by measuring the scattered intensity as a function of the angle for a series of samples. By using MALS, scattering can be simultaneously measured of several angles, which enables the determination of molecular weight from the eluent. MALS detector combined with SEC can be used to analyse the molecular weight distribution directly as polymer elutes without using internal standards. However, a value for specific refractive index increment of the polymer solution (dn/dc) is needed for each polymer-solvent system to be able to calculate the molecular weight.

8.9 SEC measurements on cellulosic materials

SEC measurements have very high requirements for the solvent used as the mobile phase. The viscosity of the solvent has to be low, it needs to be compatible with the packing material used in the column, it needs to be nearly transparent if any of the earlier mentioned detectors are used and the dissolution of the sample needs to be complete without degradation of the cell wall components.

The dissolution of a heterogeneous material like natural fibres is always an issue. Although many solvents have been demonstrated to dissolve lignocellulosic samples (Kilpeläinen et al., 2007) , there are only a few which can be used in SEC systems.

The most promising solvents for pulp samples in SEC systems are LiCl/*N,N*-dimethylacetamide (DMAc) and LiCl/1,3-dimethyl-2-imidazolidinone (DMI). Both solvent systems have been used to study wood pulps (Yanagisawa and Isogai, 2007, Karlsson and Westermark, 1996). However, incomplete dissolution of unbleached softwood pulp has been reported in the case of the LiCl/DMAc system (Sjöholm et al., 2000). The LiCl/DMAc system has also been used to analyse different kinds of kraft lignins (Sjöholm et al., 1999).

SEC measurement

SEC measurements were done by using a styrene-divinylbenzene copolymer gel packed column (KD-806M; Shodex, Japan, diameter 8 mm, length 300 mm), MALS detector (DAWNeos, λ=690 nm; Wyatt Technologies, USA) and RI detector (RID-10A; Shimadzu).

Pulp samples were activated using solvent-exchange method and dissolved into 8% LiCl/DMAc. Lignin samples were dissolved into 8% LiCl/DMI. Measurements are described in detail elsewhere (Yanagisawa et al., 2005).

8.10 Chemical compositions

Wood samples were milled with a Wiley mill and extracted with acetone to determine the extractives content. The Klason lignin and carbohydrate contents were determined according to a method by Sluiter et al. (2008). The resulting monosaccharides were measured by HPAEC (Dionex ICS-3000, CarboPac PA20 column, pulsed amperometric detection, PAD).

8.11 ESCA

The ESCA analyses of extracted and unextracted TMP pulps were carried out using an AXIS 165 electron spectrometer and monochromatic Al K_α irradiation at 100W. For elemental composition, low resolution wide spectra were recorded, using 80 eV pass energy and 1 eV step. For more detailed chemical information, carbon and oxygen were also recorded in high resolution mode, using 20 eV pass energy and 0.1 eV step. Experiments were carried out after an overnight pre-evacuation, and a reference sample of 100% cellulose paper was used as an in-situ reference, monitoring conditions in the analysis chamber during the measurement. No sample damage due to X-rays or vacuum exposure was observed. Due to the complexity of this natural material, 2-3 pieces of sample were analysed, each from at least three manually optimised locations. In curve fitting, a procedure tailored for lignocellulosic samples was applied, using four symmetric Gaussian components. Details on the experimental setup and the curve fitting used can be found in Johansson and Campbell (2004).

References

ADLER, E., BJÖRKQUIST, K. J. & HÄGGROTH, S. 1948. Über die Ursache der Farbreaktionen des Holzes. *Acta Chem. Scand.,* 2**,** 93-94.

AGARWAL, U. P. 2006. Raman imaging to investigate ultrastructure and composition of plant cell walls: distribution of lignin and cellulose in black spruce wood (*Picea mariana*). *Planta,* 224**,** 1141-1153.

AGARWAL, U. P. & RALPH, S. A. 1997. FT-Raman Spectroscopy of Wood: Identifying Contributions of Lignin and Carbohydrate Polymers in the Spectrum of Black Spruce (*Picea mariana*). *Appl. Spectrosc.,* 51**,** 1648-1655.

AGARWAL, U. P. & RALPH, S. A. Revealing organization of cellulose in wood cell walls by Raman imaging. The 14th Internationa Symposium on Wood Fibre and Pulping Chemistry, 2007 Durban, South Africa. TAPPSA, 6/25-&/28/2007.

AGARWAL, U. P. & RALPH, S. A. 2008. Determination of ethylenic residues in wood and TMP of spruce by FT-Raman spectroscopy. *Holzforschung,* 62**,** 667-675.

AGARWAL, U. P., REINER, R. & RALPH, S. 2010. Cellulose I crystallinity determination using FT–Raman spectroscopy: univariate and multivariate methods. *Cellulose,* 17**,** 721-733.

AGARWAL, U. P., WEINSTOCK, I. A. & ATALLA, R. H. 2003. FT-Raman spectroscopy for direct measurement of lignin concentrations in kraft pulps. *Tappi J.,* 2**,** 22-26.

ALTANER, C. M., TOKAREVA, E. N., JARVIS, M. C. & HARRIS, P. J. 2010. Distribution of (1→4)- β -galactans, arabinogalactan proteins, xylans and (1→3)- β -glucans in tracheid cell walls of softwoods. *Tree Physiol.,* 30**,** 782-793.

ANDERSSON, S., SERIMAA, R., PAAKKARI, T., SARANPÄÄ, P. & PESONEN, E. 2003. Crystallinity of wood and the size of cellulose crystallites in Norway spruce (*Picea abies*). *J Wood Sci,* 49**,** 531-537.

ANDERSSON, S., SERIMAA, R., TORKKELI, M., PAAKKARI, T., SARANPÄÄ, P. & PESONEN, E. 2000. Microfibril angle of Norwat spruce [*Picea abies* (L.) Karst.] compression wood: comparison of measurement techniques. *J. Wood Sci.,* 46**,** 343-349.

ATALLA, R. H. 1976. Raman Spectral Studies of Polymorphy in Cellulose. Part I: Celluloses I and II. *Appl. Polym. Symp.,* 28**,** 659-669.

ATALLA, R. H. & AGARWAL, U. P. 1985. Raman Microprobe Evidence for Lignin Orientation in the Cell Walls of Native Woody Tissue. *Science,* 227**,** 636-638.

ATALLA, R. H. & AGARWAL, U. P. 1986. Recording Raman spectra from plant cell walls. *J. Raman Spectrosc.,* 17**,** 229-231.

ATALLA, R. H., BRADY, J. W., MATTHEWS, J. F., DING, S.-Y. & HIMMEL, M. E. 2009. *Structures of Plant Cell Wall Celluloses* In Biomass Recalcitrance: Deconstructing the Plant Cell Wall for Bioenergy, Blackwell Publishing Ltd.

ATALLA, R. H. & VANDERHART, D. L. 1984. Native Cellulose: A Composite of Two Distinct Crystalline Forms. *Science,* 223**,** 283-285.

ATALLA, R. H., WHITMORE, R. E. & HEIMBACH, C. J. 1980. Raman Spectral Evidence for Molecular Orientation in Native Cellulosic Fibers. *Macromolecules,* 13**,** 1717-1719.

BALEY, C. 2004. Influence of kink bands on the tensile strength of flax fibers. *J. Mater. Sci.,* 39**,** 331-334.

BATTISTA, O. A. 1950. Hydrolysis and Crystallization of Cellulose. *Ind. Eng. Chem.,* 42**,** 502-507.

BERGANDER, A. & SALMÉN, L. 2002. Cell wall properties and their effects on the mechanical properties of fibers. *J. Mater. Sci.,* 37**,** 151-156.

BJÖRKMAN, A. 1956. Studies on finely divided wood. Part 1. Extraction of lignin with neutral solvents. *Svensk. Papperstidn.,* 59**,** 477-485.

BLACKBURN, R. S. 2005. *Biodegradable and sustainable fibres,* Cambridge :, Woodhead.

BLAKE, A., MARCUS, S., COPELAND, J., BLACKBURN, R. & KNOX, J. 2008. In situ analysis of cell wall polymers associated with phloem fibre cells in stems of hemp, <i>Cannabis sativa</i> L. *Planta,* 228**,** 1-13.

BOERJAN, W., RALPH, J. & BAUCHER, M. 2003. Lignin Biosynthesis. *Annu. Rev. Plant biol.,* 54**,** 519-546.

BURGERT, I., FRÜHMANN, K., KECKES, J., FRATZL, P. & STANZL-TSCHEGG, S. 2004. Structure–function relationships of four compression wood types: micromechanical properties at the tissue and fibre level. *Trees Struct. Funct.,* 18**,** 480-485.

CAPANEMA, E. A., BALAKSHIN, M. Y. & CHEN, C.-L. 2004. An improved procedure for isolation of residual lignins from hardwood kraft pulps. *Holzforschung,* 58**,** 464-472.

CHARLET, K., JERNOT, J. P., EVE, S., GOMINA, M. & BRÉARD, J. 2010. Multi-scale morphological characterisation of flax: From the stem to the fibrils. *Carbohyd. Polym.,* 82**,** 54-61.

CÓTE, W. A., DAY JR., A. C. & TIMELL, T. E. 1968. Distribution in Normal and Compression Wood of Tamarak. *Wood Sci. Technol.,* 2**,** 13-37.

DA SILVA PEREZ, D. & VAN HEININGEN, A. R. P. 2002. Determination of cellulose degree of polymerization in chemical pulps by viscometry. *Seventh European Workshop on Lignocellulosics and Pulp.* Turku, Finland.

DAVIDSON, T. C., NEWMAN, R. H. & RYAN, M. J. 2004. Variations in the fibre repeat between samples of cellulose I from different sources. *Carbohyd Res,* 339**,** 2889-2893.

DAVIES, G. C. & BRUCE, D. M. 1998. Effect of Environmental Relative Humidity and Damage on the tensile Properties of flax and Nettle Fibers. *Text. Res. J.,* 68**,** 623-629.

DAY, A., RUEL, K., NEUTELINGS, G., CRÔNIER, D., DAVID, H., HAWKINS, S. & CHABBERT, B. 2005. Lignification in the flax stem: evidence for an unusual lignin in bast fibers. *Planta,* 222**,** 234-245.

DISSANAYAKE, N. P. J., SUMMERSCALES, J., GROVE, S. M. & SINGH, M. M. 2009a. Energy use in production of flax fiber for the reinforcement of composites. *J. Nat. Fiber.,* 6**,** 331-346.

DISSANAYAKE, N. P. J., SUMMERSCALES, J., GROVE, S. M. & SINGH, M. M. 2009b. Life Cycle Impact Assesment of Flax Fibre for the Reinforcement of Composites. *J. Biobased Mater. Bio. ,* 3**,** 245-248.
DONALDSON, L. 2007. Cellulose microfibril aggregates and their size variation with cell wall type. *Wood Sci. Technol.,* 41**,** 443-460.
DONALDSON, L. A. 2008. Microfibril angle: Measurement, variation and relationships - A review. *IAWA J.,* 29**,** 345-386.
DONALDSON, L. A., SINGH, A. P., YOSHINAGA, A. & TAKABE, K. 1999. Lignin distribution in mild compression wood of *Pinus radiata*. *Can. J. Bot.,* 77**,** 41-50.
EDER, M. & BURGERT, I. 2010. *2.2 Natural Fibres - Function in Nature*, John Wiley & Sons, Ltd.
EICHHORN, S. J., HUGHES, M., SNELL, R. & MOTT, L. 2000. Strain induced shifts in the Raman spectra of natural cellulose fibers. *J. Mater. Sci. Lett.,* 19**,** 721-723.
EICHHORN, S. J. & YOUNG, R. J. 2001. The Young's modulus of a microcrystalline cellulose. *Cellulose,* 8**,** 197-207.
EICHHORN, S. J., YOUNG, R. J., DAVIES, R. J. & RIEKEL, C. 2003. Characterisation of the microstructure and deformation of high modulus cellulose fibres. *Polymer,* 44**,** 5901-5908.
EVANS, R. & ILIC, J. 2001. Rapid Prediction of Wood stiffness from Microfibril Angle and Density. *For. Prod. J.,* 51**,** 53-57.
EVANS, R. & WALLIS, A. F. A. 1989. Cellulose molecular weights determined by viscometry. *J. App. Polym. Sci.,* 37**,** 2331-2340.
FAHLÉN, J. & SALMÉN, L. 2004. Pore and Matrix Distribution in the Fiber Wall Revealed by Atomic Force Microscopy and Image Analysis. *Biomacromolecules,* 6**,** 433-438.
FERGUS, B. J., PROCTER, A. R., SCOTT, J. A. N. & GORING, D. A. I. 1969. The Distribution of Lignin in Sprucewood as Determined by Ultraviolet Microscopy. *Wood Sci. Technol.,* 3**,** 117-138.
FERNANDO, D. & DANIEL, G. 2008. Exploring Scots pine fibre development mechanisms during TMP processing: Impact of cell wall ultrastructure (morphological and topochemical) on negative behaviour. *Holzforschung,* 62**,** 597-607.
GERE, J. M. 1997. *Mechanics of materials,* Boston, PWS Publishing.
GIERLINGER, N., LUSS, S., KÖNIG, C., KONNERTH, J., EDER, M. & FRATZL, P. 2010. Cellulose microfibril orientation of Picea abies and its variability at the micron-level determined by Raman imaging. *J Exp. Bot.,* 61**,** 587-595.
GIERLINGER, N. & SCHWANNINGER, M. 2006. Chemical Imaging of Poplar Wood Cell Walls by Confocal Raman Microscopy. *Plant Physiol.,* 140**,** 1246-1254.
GIERLINGER, N., SCHWANNINGER, M., REINECKE, A. & BURGERT, I. 2006. Molecular Changes during Tensile Deformation of Single Wood Fibers Followed by Raman Microscopy. *Biomacromolecules,* 7**,** 2077-2081.
GORSHKOVA, T. A., SALNIKOV, V. V., POGODINA, N. M., CHEMIKOSOVA, S. B., YABLOKOVA, E. V., ULANOV, A. V., AGEEVA, M. V., VAN DAM, J. E. G. & LOZOVAYA, V. V. 2000. Composition and Distribution of Cell Wall

Phenolic Compounds in Flax (Linum usitatissimum L.) Stem Tissues. *Ann. Bot.,* 85**,** 477-486.
GUERRA, A., FILPPONEN, I., LUCIA, L. A. & ARGYROPOULOS, D. S. 2006. Comparative Evaluation of Three Lignin Isolation Protocols for Various Wood Species. *J. Agric. Food Chem.,* 54**,** 9696-9705.
GURNAGUL, N., D.H., P. & PAICE, M. G. 1992. The effect of cellulose degradtion on the strength of wood pulp fibres. *Nord. Pulp Pap. Res. J.,* 3**,** 152-154.
HALTTUNEN, M., VYÖRYKKÄ, J., HORTLING, B., TAMMINEN, T., BATCHELDER, D., ZIMMERMANN, A. & VUORINEN, T. 2001. Study of Residual Lignin in Pulp by UV Resonance Raman Spectroscopy. *Holzforschung,* 55**,** 631-638.
HEARLE, J. W. S. 1958. A fringed fibril theory of structure in crystalline polymers. *J. Polym. Sci.,* 28**,** 432-435.
HENRIKSSON, G., LAWOKO, M., MARTIN, M. E. E. & GELLERSTEDT, G. 2007. Lignin-carbohydrate network in wood and pulps: A determinant for reactivity. *Holzforschung,* 61**,** 668-674.
HULL, D. & CLYNE, T. W. 1996. *An introduction to composite materials*, Cambridge University Press.
HULT, E.-L., LARSSON, P. T. & IVERSEN, T. 2001. A CP/MAS 13C-NMR study of supramolecular changes in cellulose and hemicelluloses structure during kraft pulping. *Nord. Pulp Pap. Res. J.,* 16**,** 33-39.
HÅKANSON, H., AHLGREN, P. & GERMFÅRD, U. 2005. The degree of disorder in hardwood kraft pulps studied by means of LODP. *Cellulose,* 12**,** 327-335.
HÄNNINEN, T. & HUGHES, M. 2010. *19.1 Historical, Contemporary and Future Applications* In Industrial Applications of Natural Fibres: Structure, Properties and Technical Applications, John Wiley & Sons, Ltd.
IRVINE, G. M. 1985. The significance of the glass transition of lignin in thermomechanical pulping. *Wood Sci. Technol.,* 19**,** 139-149.
ISOGAI, A., ISHIZU, A. & NAKANO, J. 1989. Residual Lignin and Hemicellulose in Wood Cellulose. Analysis Using New Permethylation Method. *Holzforschung,* 43**,** 333-338.
JIN, Z., KATSUMATA, K. S., LAM, T. B. T. & IIYAMA, K. 2006. Covalent linkages between cellulose and lignin in cell walls of coniferous and nonconiferous woods. *Biopolymers,* 83**,** 103-110.
JOHANSSON, L.-S. 2002. Monitoring Fibre Surfaces with XPS in Papermaking Processes. *Mikrochim. Acta,* 138**,** 217-223.
JOHANSSON, L.-S. & CAMPBELL, J. M. 2004. Reproducible XPS on biopolymers: cellulose studies. *Surf. Interface Anal.,* 36**,** 1018-1022.
JOUTSIMO, O. & ROBERTSEN, L. 2004. The effect of mechanical treatment on softwood kraft pulp fibers. *Pap. Puu,* 86**,** 359-364.
JÄÄSKELÄINEN, A.-S., SAARIAHO, A.-M. & VUORINEN, T. 2005. Quantification of Lignin and Hexenuronic Acid in Bleached Hardwood Kraft Pulps: A New Calibration Method for UVRR Spectroscopy and Evaluation of the Conventional Methods. *J. Wood. Chem. Technol.,* 25**,** 51 - 65.

JÄÄSKELÄINEN, A.-S., SAARIAHO, A.-M., VYÖRYKKÄ, J., VUORINEN, T., MATOUSEK, P. & PARKER, A. W. 2006. Application of UV-Vis and resonance Raman spectroscopy to study bleaching and photoyellowing of thermomechanical pulps. *Holzforschung,* 60**,** 231-238.

KANTOLA, M. & KÄHKÖNEN, M. 1963. Small-angle X-Ray Investigation of the Orientation of Crystallites in Finnish Coniferous and Deciduos Wood fibers. *Ann. Acad. Scient. Fenn.,* A VI 137**,** 3-14.

KANTOLA, M. & SEITSONEN, S. 1961. X-Ray Orientation Investigations on finnish Conifers. *Ann. Acad. Scient. Fenn.,* A VI 80**,** 3-15.

KARLSSON, O. & WESTERMARK, U. 1996. Evidence for Chemical Bonds Between Lignin and Cellulose in Kraft Pulps. *J. Pulp Pap. Sci.,* 22**,** J397-J401.

KARNIS, A. 1994. The Mechanism of Fibre Development in Mechanical Pulping. *J. Pulp Pap. Sci.,* 20**,** J280-J287.

KECKES, J., BURGERT, I., FRUHMANN, K., MULLER, M., KOLLN, K., HAMILTON, M., BURGHAMMER, M., ROTH, S. V., STANZL-TSCHEGG, S. & FRATZL, P. 2003. Cell-wall recovery after irreversible deformation of wood. *Nat. Mater.,* 2**,** 810-813.

KEKKONEN, P. M., TELKKI, V.-V. & JOKISAARI, J. 2009. Determining the Highly Anisotropic Cell Structures of *Pinus sylvestris* in three Orthogonal directions by PGSTE NMR of Adsorbed Water and Methane. *J. Phys. Chem. B,* 113**,** 1080-1084.

KEUNECKE, D., EDER, M., BURGERT, I. & NIEMZ, P. 2008. Micromechanical properties of common yew (*Taxus baccata*) and Norway spruce (*Picea abies*) transition wood fibers subjected to longitudinal tension. *J. Wood. Sci.,* 54**,** 420-422.

KIBBLEWHITE, R. P. 1999. Designer fibres for improved papers through exploiting genetic variation in wood microstructure. *Appita J.,* 52**,** 429-435, 440.

KIHARA, M., TAKAYAMA, M., WARIISHI, H. & TANAKA, H. 2002. Determination of the carbonyl groups in native lignin utilizing Fourier transform Raman spectroscopy. *Spectrochim. Acta Part A,* 58**,** 2213-2221.

KILPELÄINEN, I., XIE, H., KING, A., GRANSTROM, M., HEIKKINEN, S. & ARGYROPOULOS, D. S. 2007. Dissolution of Wood in Ionic Liquids. *J. Agric. Food Chem.,* 55**,** 9142-9148.

KLEMM, D., PHILIPP, B., HEINZE, T., HEINZE, U. & WAGENKNECHT, W. 2004. *Comprehensive Cellulose Chemistry: Fundamentals and Analytical Methods, Vol. 1*, Wiley-VCH Verlag GmbH & Co. KGaA.

KOLJONEN, K., ÖSTERBERG, M., KLEEN, M., FUHRMANN, A. & STENIUS, P. 2004. Precipitation of lignin and extractives on kraft pulp: effect onsurface chemistry, surface morphology and paper strength. *Cellulose,* 11**,** 209-224.

KONTTURI, E. & VUORINEN, T. 2006. Fibre surface and strength of a fibre network. *Holzforschung,* 60**,** 691-693.

LAWOKO, M., HENRIKSSON, G. & GELLERSTEDT, G. 2005. Structural Differences between the Lignin-Carbohydrate Complexes Present in Wood and in Chemical Pulps. *Biomacromolecules,* 6**,** 3467-3473.

LEPPÄNEN, K., ANDERSSON, S., TORKKELI, M., KNAAPILA, M., KOTELNIKOVA, N. & SERIMAA, R. 2009. Structure of cellulose and microcrystalline cellulose from various wood species, cotton and flax studied by X-ray scattering. *Cellulose,* 16**,** 999-1015.

LI, J., MARTIN-SAMPEDRO, R., PEDRAZZI, C. & GELLERSTEDT, G. 2011. Fractionation and characterization of lignin-carbohydrate complexes (LCCs) from eucalyptus fibers. *Holzforschung,* 65**,** 43-50.

LI, K., TAN, X. & YAN, D. 2006. The middle lamella remainders on the surface of various mechanical pulp fibres. *Surf. Interface Anal.,* 38**,** 1328-1335.

MACKAY, J. J., PRESNELL, T., JAMEEL, H., TANEDA, H. & O'MALLEY, M. D. 1999. Modified lignin and delignifaction wit a CAD-deficient loblolly pine. *Holzforschung,* 53**,** 403-410.

MACLEOD, J. M. 1990. Basket Cases: Kraft-Pulp Strength Variability Within a Batch Digester. *Tappi J.,* 73**,** 185-190.

MALAWER, E. G. & SENAK, L. 2004. Introduction to Size Exclusion Chromatography. *In:* WU, C.-S. (ed.) *Handbook of Size Exclusion Chromatography and Related Techniques.* 2nd edition ed. New York: Marcel Dekker.

MARK, H. 1940. Intermicellar Hole and Tube System in Fiber Structure. *J. Phys. Chem.,* 44**,** 764-788.

MAST, S. W., DONALDSON, L., TORR, K., PHILLIPS, L., FLINT, H., WEST, M., STRABALA, T. J. & WAGNER, A. 2009. Exploring the Ultrastructural Localization and Biosynthesis of β(1,4)-Galactan in Pinus radiata Compression Wood. *Plant Physiol.,* 150**,** 573-583.

MAXIMOVA, N., ÖSTERBERG, M., KOLJONEN, K. & STENIUS, P. 2001. Lignin adsorption on cellulose fibre surfaces: Effect on surface chemistry, surface morphology and paper strenght. *Cellulose,* 8**,** 113-125.

MCCREERY, R. L. 2000. *Raman Spectroscopy for Chemical Analysis,* United States of America, John Wiley & Sons, Inc.

MCLEAN, J. P., EVANS, R. & MOORE, J. R. 2010. Predicting the longitudinal modulus of elasticity of Sitka spruce from cellulose orientation and abundance. *Holzforschung,* 64**,** 495-500.

MESHITSUKA, G. & ISOGAI, A. 1996. Chemical structures of cellulose, hemicelluloses and lignin. *In:* HON, D. N.-S. (ed.) *Chemical Modification of Lignocellulosic Materials.* New Yourk: Dekker.

MÜSSIG, J., FISCHER, H., GRAUPNER, N. & DRIELING, A. 2010. *13 Testing Methods for Measuring Physical Properties and Mechanical Fibre Properties (Plant and Animal Fibres)* In Industrial Applications of Natural Fibres: Structure, Properties and Technical Applications, John Wiley & Sons, Ltd.

NISHIYAMA, Y., KIM, U.-J., KIM, D.-Y., KATSUMATA, K. S., MAY, R. P. & LANGAN, P. 2003. Periodic Disorder along Ramie Cellulose Microfibrils. *Biomacromolecules,* 4**,** 1013-1017.

OLSSON, A.-M. & SALMÉN, L. 1997. The effect of lignin composition on the viscoelastic properties of wood. *Nord. Pulp Pap. Res. J.,* 12**,** 140-144.

PAGE, D. H. 1983. The Origin of the Differences Between Sulphite and Kraft Pulps. *J. Pulp. Pap. Sci.,* 9**,** TR 15 - TR 20.

PAGE, D. H., EL-HOSSEINY, F., WINKLER, K. & BAIN, R. 1972. The mechanical properties of single wood-pulp fibres. Part I: A new approach. *Pulp Pap. Can.,* 73**,** 72-77.

PAGE, D. H. & SETH, R. S. 1980. The elastic modulus of paper II. The importance of fiber modulus, bonding, and fiber length. *Tappi,* 63**,** 113-116.

PENG, F. & WESTERMARK, U. 1997. Distribution of Coniferyl Alcohol and Coniferaldehyde Groups in the Cell Wall of Spruce Fibres. *Holzforschung,* 51**,** 531-536.

RAUVANTO, I., PERE, J. & HENRICSON, K. 2006. Fibre damage in unbleached pulp - The effect of hemicelluloses and lignin on the susceptibility of fibres to damage during oxygen delignification. *Nord. Pulp Pap. Res. J.,* 21**,** 328-335.

REIS, D. & VIAN, B. 2004. Helicoidal pattern in secondary cell walls and possible role of xylans in their construction. *C. R. Biol.,* 327**,** 785-790.

REME, P. A. & HELLE, T. 2001. On the difference in response to refining between Norway Spruce and Scots Pine. *Pap. Puu,* 83**,** 58-61.

ROBERTSEN, L. & JOUTSIMO, O. 2005. The effect of mechanical treatment on kraft pulps produced from different softwood materials. *Pap. Puu,* 87**,** 111-115.

ROMHÁNY, G., KARGER-KOCSIS, J. & CZIGÁNY, T. 2003. Tensile fracture and failure behavior of technical flax fibers. *J. App. Polym. Sci.,* 90**,** 3638-3645.

ROWELL, R. M. 2008. Natural fibres: types and properties. *In:* PICKERING, K. L. (ed.) *Properties and Performance of Natural-Fibre Composites.* Cambridge, UK: Woodhead Publishing Limited.

RYDHOLM, S. A. 1965. *Pulping processes,* New York :, Interscience Publishers.

SAARIAHO, A.-M., ARGYROPOULOS, D. S., JÄÄSKELÄINEN, A.-S. & VUORINEN, T. 2005. Development of the partial least squares models for the interpretation of the UV resonance Raman spectra of lignin model compounds. *Vibrat. Spec.,* 37**,** 111-121.

SAKAKIBARA, A. & SANO, Y. 1996. Chemistry of Lignin. *In:* HON, D. N.-S. (ed.) *Chemical Modification of Lignocellulosic Materials.* New Yourk: Dekker.

SALMÉN, L. & BERGSTRÖM, E. 2009. Cellulose structural arrangement in relation to spectral changes in tensile loading FTIR. *Cellulose,* 16**,** 975-982.

SALMÉN, L. & OLSSON, A.-M. 1998. Interaction Between Hemicelluloses, Lignin and Cellulose: Structure-Property Relationships. *J. Pulp Pap. Sci.,* 24**,** 99-102.

SÁREN, M.-P., SERIMAA, R., ANDERSSON, S., PAAKKARI, T., SARANPÄÄ, P. & PESONEN, E. 2001. Structural Variation of Tracheids in Norway Spruce (*Picea abies* [L] Karst.). *J. Struct. Biol.,* 139**,** 101-109.

SCHENZEL, K. & FISCHER, S. 2001. NIR FT Raman Spectroscopy–a Rapid Analytical Tool for Detecting the Transformation of Cellulose Polymorphs. *Cellulose,* 8**,** 49-57.

SCHENZEL, K., FISCHER, S. & BRENDLER, E. 2005. New Method for Determining the Degree of Cellulose I Crystallinity by Means of FT Raman Spectroscopy. *Cellulose,* 12**,** 223-231.

SCHMIDT, M., SCHWARTZBERG, A., PERERA, P., WEBER-BARGIONI, A., CARROLL, A., SARKAR, P., BOSNEAGA, E., URBAN, J., SONG, J., BALAKSHIN, M., CAPANEMA, E., AUER, M., ADAMS, P., CHIANG, V. &

SCHUCK, P. 2009. Label-free in situ imaging of lignification in the cell wall of low lignin transgenic <i>Populus trichocarpa</i&gt. *Planta,* 230**,** 589-597.
SEDEROFF, R. R., MACKAY, J. J., RALPH, J. & HATFIELD, R. D. 1999. Unexpected variation in lignin. *Curr. Opin. Plant Biol.,* 2**,** 145-152.
SETH, R. S. 2006. The importance of fibre straightness for pulp strength. *Pulp Pap. Can.,* 107**,** 34-41.
SETH, R. S. & PAGE, D. H. 1988. Fiber properties and tearing resistance. *Tappi J.,* 71**,** 103-107.
SIXTA, H. 2008. *Handbook of pulp*, Wiley-VCH Verlag GmbH.
SJÖHOLM, E., GUSTAFSSON, K., BERTHOLD, F. & COLMSJÖ, A. 2000. Influence of the carbohydrate compositionon the molecular weight distribution of kraft pulps. *Carbohyd. Polym.,* 41**,** 1-7.
SJÖHOLM, E., GUSTAFSSON, K. & COLMSJÖ, A. 1999. Size Exclusion Chromatography of Lignins using Lithium Chloride/N,N-Dimethylacetamide as Mobile Phase. II. Dissolved and Residual Pine Kraft Lignins. *J. Liq. Chrom. & Rel. Technol.,* 22**,** 2837-2854.
SJÖSTRÖM, E. 1993. *Wood Chemistry - Fundamentals and Applications,* London, U.K., Academic Press, Inc.
SLUITER, A., HAMES, B., RUIZ, R., SCARLATA, C., SLUITER, B., TEMPLETON, D. & CROCKER, D. 2008. Determination of Structural Carbohydrates and Lignin in Biomass. *NREL Laboratory Analytical Procedure (LAP).*
SMITH, E. & DENT, G. 2005. Introduction, Basic Theory and Principles. *Modern Raman spectroscopy - A Practical Approach.* Chichester, England: John Wiley & Sons Ltd.
TAKAYAMA, M., JOHJIMA, T., YAMANAKA, T., WARIISHI, H. & TANAKA, H. 1997. Fourier transform Raman assignment of guaiacyl and syringyl marker bands for lignin determination. *Spectrochim. Acta Part A,* 53**,** 1621-1628.
TANAKA, F., KOSHIJIMA, T. & OKAMURA, K. 1981. Characterization of cellulose in compression and opposite woods of a *Pinus densiflora* tree grown under the influence of strong wind. *Wood Sci. Technol.,* 15**,** 265-273.
TANAKA, M. & YOUNG, R. 2006. Review Polarised Raman spectroscopy for the study of molecular orientation distributions in polymers. *J. Mater. Sci.,* 41**,** 963-991.
TENKANEN, M., TAMMINEN, T. & HORTLING, B. 1999. Investigation of lignin-carbohydrate complexes in kraft pulps by selective enzymatic treatments. *Appl. Microbiol. Biot.,* 51**,** 241-248.
TERASHIMA, N., KITANO, K., KOJIMA, M., YOSHIDA, M., YAMAMOTO, H. & WESTERMARK, U. 2009. Nanostructural assembly of cellulose, hemicellulose, and lignin in the middle layer of secondary wall of ginkgo tracheid. *J. Wood Sci.,* 55**,** 409-416.
THYGESEN, L., EDER, M. & BURGERT, I. 2007. Dislocations in single hemp fibres—investigations into the relationship of structural distortions and tensile properties at the cell wall level. *J. Mater. Sci.,* 42**,** 558-564.
TIMELL, T. E. 1986. *Compression wood in gymnosperms,* Berlin, Germany, Springer-Verlag.

VANDERHART, D. L. & ATALLA, R. H. 1984. Studies of microstructure in native celluloses using solid-state carbon-13 NMR. *Macromolecules,* 17**,** 1465-1472.

WARDROP, A. B. 1964. Cellular Differentiation in Xylem. *In:* CÓTE, W. A. (ed.) *Cellular Ultrastructure of Woody Plants.* New York: Syracuse University Press.

WHITING, P. & GORING, D. 1982. Chemical characterization of tissue fractions from the middle lamella and secondary wall of black spruce tracheids. *Wood Sci. Technol.,* 16**,** 261-267.

VIËTOR, R. J., NEWMAN, R. H., HA, M.-A., APPERLEY, D. C. & JARVIS, M. C. 2002. Conformational features of crystal-surface cellulose from higher plants. *Plant J.,* 30**,** 721-731.

WILEY, J. H. & ATALLA, R. H. 1987. Band assignments in the raman spectra of celluloses. *Carbohyd. Polym.,* 160**,** 113-129.

YANAGISAWA, M. & ISOGAI, A. 2007. Size exclusion chromatographic and UV-VIS absorption analyses of unbleached and bleached softwood kraft pulps using LiCl/1,3-dimethyl-2-imidazolidinone as a solvent. *Holzforschung,* 61**,** 236-241.

YANAGISAWA, M., SHIBATA, I. & ISOGAI, A. 2005. SEC-MALLS analysis of softwood kraft pulp using LiCl/1,3-dimethyl-2-imidazolidinone as an eluent. *Cellulose,* 12**,** 151-158.

YANG, J. L. & EVANS, R. 2003. Prediction of MOE of eucalyptu wood from microfibril angle and density. *Holz Roh. Werkst.,* 61.

Tuomas Hänninen Studies on the ultrastructure of natural fibres and its effects on the fibre utilization Aalto University

Aalto-DD 116/2011

BUSINESS + ECONOMY

ART + DESIGN + ARCHITECTURE

SCIENCE + TECHNOLOGY

CROSSOVER

DOCTORAL DISSERTATIONS

ISBN 978-952-60-4359-3 (pdf)
ISBN 978-952-60-4358-6
ISSN-L 1799-4934
ISSN 1799-4942 (pdf)
ISSN 1799-4934

Aalto University
School of Chemical Technology
Department of Forest Products Technology
www.aalto.fi